Additional Benefit Estimates of Synthetic Vision Technology

NS014S1

June 2001

Robert Hemm
David Lee
Virginia Stouffer
Ashleigh Gardner

Additional Benefit Estimates of Synthetic Vision Technology

NS014S1

June 2001

Robert Hemm
David Lee
Virginia Stouffer
Ashleigh Gardner

Prepared pursuant to National Aeronautics and Space Administration Contract POL 70525D. The views expressed here are those of the Logistics Management Institute at the time of issue but not necessarily those of NASA.

LOGISTICS MANAGEMENT INSTITUTE
2000 CORPORATE RIDGE
MCLEAN, VIRGINIA 22102-7805

Contents

FIGURES

TABLES

Chapter 1
Overview And Summary Results

This chapter briefly defines synthetic vision (SV) technology, discusses the methods used to estimate benefits, and summarizes the results.

BACKGROUND

Synthetic vision implies the presentation to the pilot of a computer-generated view of the external environment. The SV system presentation is completely artificial. It typically is based on static geographical and cultural data[1] supplemented by dynamic traffic information. Current experimental implementations of SVS use Global Positioning Satellite (GPS) data to register the data base information dynamically to the aircraft's position and altitude. Supplemental sensors may be used to confirm the GPS position data or provide additional data (e.g., other aircraft, weather events, ground equipment). Synthetic vision systems can use both head-up and head-down displays, but the current concept focuses on a head-down display. Displays can include an artificial out-of-the-window view (in all directions) or any number of symbolic and map presentations.

In a broad sense, SV includes all artificial information that represents the real world. For example, the "wire frame" runway edge symbols generated from instrument landing system (ILS) data that are featured on some current guidance systems can be considered synthetic vision. For this study; however, we define synthetic vision as the display of comprehensive geographic, cultural, and tactical data.

To avoid a common source of confusion, we note here the difference between "enhanced" vision (EV) and "synthetic" vision. Enhanced vision refers to the direct presentation to the aircrew of data from weather- and darkness-penetrating sensors such as radar or forward-looking infrared (FLIR). The data presented are derived from the current environment and not from a computer data base. EV systems can use both head-down and head-up displays. EV displays are limited to the field-of-regard of the sensor.

[1] Cultural data include obstacles such as buildings, and features such as runways, taxiways, and gates.

In our previous analysis we estimated the benefits of SV for 10 major airports. [2] We made the estimates using airport capacity and delay models of the type developed for estimating the benefits of the NASA Terminal Area Productivity program. In our current effort, we addressed the following tasks:

- Update the current capacity and delay analysis based on industry input
- Estimate the benefits of reducing ceiling and visibility minimums for arrivals and departures at additional airports
- Analyze SVS economic benefits for feeder and cargo operations
- Analyze SVS economic benefits for business operations

To date, we have received no industry inputs, so we have not updated the previous results. We anticipate future changes may be required if SV test results support new values for model input parameters.

INDIVIDUAL AIRPORT ANALYSIS

The potential set of additional airports included Juneau (JNU), San Diego (SAN), Eagle County/Vail (EGE), Washington Reagan (DCA), Reno (RNO), Salt Lake City (SLC), San Francisco (SFO), and Las Vegas (LAS). Sacramento (SMF) was added to the list while we were working on the task. The airports we analyzed for this report were JNU, SAN, SMF, DCA, and EGE.

We developed three new models for the analysis. We used a single-runway model, based on previous work, but containing new features, for JNU, SAN, and SMF. We developed an airport-unique capacity and delay model set for DCA. Finally, we developed a "simplified" delay analysis for EGE.

Description of the Technology Set

In the airport analysis, we compare the benefits for three SV technologies: SV1, SV2, and SV3, to a 2005 baseline (BL) technology. The technologies are defined by their capabilities rather than by their hardware and software content. A discussion of the selection of the sets and their capabilities is contained in our previous report. The capabilities of the technologies are summarized in Table 1-1.

[2] *Benefit Estimates of Synthetic Vision Technology*, R. Hemm, NS002S1, July 2000. located at http://avsp.larc.nasa.gov/SV%20Benefits/Benefit_Eatimates_of_SV.pdf

Table 1-1. Technology Performance Assumptions

Technology Set	Departure Minimum	Arrival Minimums Ceiling/Visibility*	Comments
BL	700	Airport Approach Plate Minimums	• Cat II and Cat III operations on Cat II runways with current Cat III ceiling and visibility minimums
SV1	700	0 / 600 (no 300 ft taxi capability)	• Cat II and Cat III operations on all runways with reduced Cat III ceiling and visibility minimums • Converging and circling operations in all IFR
SV2	300	0 / 300	• Cat II and Cat III operations on all runways with reduced Cat III ceiling and visibility minimums. • Converging and circling operations in all IFR. • Reduced low visibility runway occupancy time.
SV3	300	0 / 300	• Cat II and Cat III operationas on all runways with reduced Cat III ceiling and visibility minimums • Converging and circling operations in all IFR • Reduced separations • Reduced low visibility runway occupancy time. • Independent IFR operations on parallel runways with spacing ≥ 2500 ft.

** ceiling = Decision Height (DH) or Alert Height (AH) in feet*
visibility = Runway Visual Range (RVR) in feet

Results for DCA, SAN, JNU and SMF

Table 1-2 and Figure 1-1 display the average annual delay-reduction benefits of the three SV technology sets compared BL for DCA, SAN, JNU, and SMF, based on the 10 years from 2006 through 2015. The JNU benefits are for a baseline that uses Alaska Airline developed LDA-2/3 procedure minimums instead of those published in the TERPs.[3] Alaska Airlines also uses required navigation performance (RNP) procedures that provide results similar to SV1. A more detailed comparison of JNU benefits, including an estimate specifically for Alaska Airlines is contained in Chapter 2.

[3] LDA: localizer-type decision aid. Alaska Airlines developed reduced minimum LDA procedures for Juneau. We assume that other major carriers servicing JNU would do the same. In addition, Alaska Airlines has developed unique, reduced-minimum, required navigation performance procedures using GPS, inertial navigation, and head-up displays that enable instrument approaches to Runway 26.

TERPS: terminal area radar procedures. These are FAA instrument procedures published for general use. At most airports TERPS are the only procedures used.

Table 1-2. Airport Benefits Summary

Average Annual Minutes Saved (in millions)					
Technology	Total	DCA	SAN	JNU	SMF
SV1	2.8	0.84	1.80	0.21	0.02
SV2	2.9	0.85	1.86	0.21	0.14
SV3	3.1	0.87	2.03	0.21	0.14
Average Annual 1999 Constant Dollar Savings (in millions)					
Technology	Total	DCA	SAN	JNU	SMF
SV1	104	30.8	66.0	7.6	0.6
SV2	107	31.1	68.5	7.7	5.0
SV3	114	31.9	74.5	7.7	5.1

Figure 1-1. Average Annual Savings

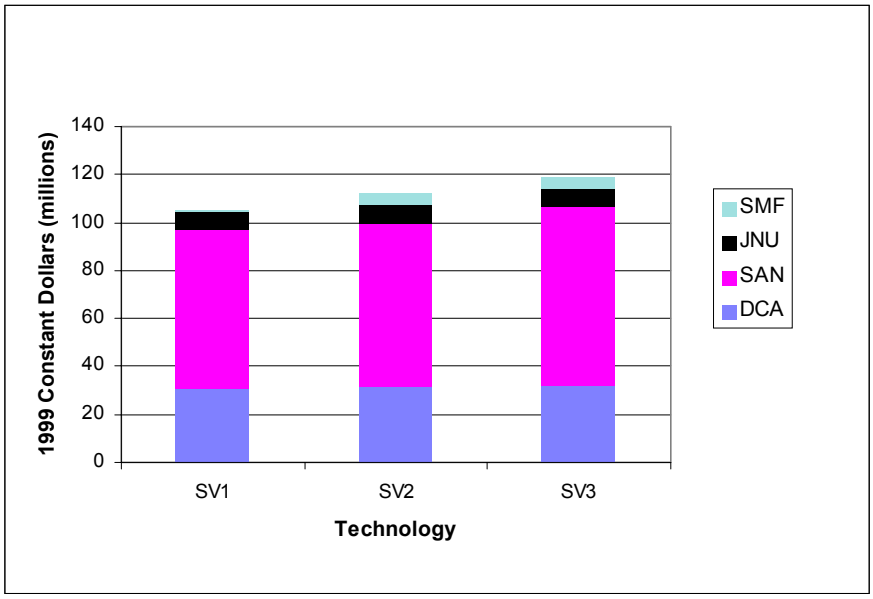

Table 1-1 and Figure 1-1 indicate that the primary benefits at JNU, SAN, and DCA are gained with the SV1capability to use runways and approaches that are currently limited by high ceiling and high visibility minimums during inclement weather conditions. SV1 also eliminates missed approaches at SAN. Additional SV2 visibility minimum reductions to 300 feet for arrivals and departures, and SV3 reductions in miles-in-trail spacing provide marginal improvements. The benefits for SMF are relatively small, and appear to derive from the SV2 reduction of the visibility minimum from 600 feet to 300 feet.

EGE Results

Estimating benefits for the Eagle County/Vail airport presented an interesting problem because the scheduled demand is extremely low. Our normal practice of

estimating the cost of delays according to demand does not provide helpful information. To investigate the benefits at EGE we elected an analysis that displays the expected delay for an arrival and departure scheduled for a particular hour of a particular month. In keeping with the low demand, we assumed that the airport has adequate capacity whenever weather conditions are above minimums and has zero capacity when below minimums. The delay model assumes that one aircraft is scheduled to arrive each hour and leave the following hour. Arrivals are delayed by weather only, but departures can be delayed either by weather or by lack of an aircraft. The model output includes both the annual delay results and the delay as a function of hour and month. We found that implementation of SV1 technology essentially eliminates delays at EGE.

NOISE REDUCTION ANALYSIS

We ran the Aviation System Analysis Capability (ASAC) DCA noise model to determine how SV technology might reduce noise. We made two analyses. In the first, we compared the current average operations mix of the airport to 100 percent use of the noise abatement, visual flight rules (VFR), river routes. In the second, we compared the noise on the IFR routes to the river routes. The results are discussed in Chapter 7.

BUSINESS AIRCRAFT ANALYSIS

We estimated the potential SV benefit to business aircraft using a modified version of the LMINET delay model. The LMINET model used was developed to analyze the Small Aircraft Transportation System (SATS) and includes a network of 2,865 airports. We developed a demand schedule for the SATS network in a separate task.[4] For this estimate, we considered the demand due to twin turboprops as representing business aircraft. As with the EGE analysis, we considered the capacity as being infinite when an airport was open, and zero when it was below minimums.

We ran the following six cases; the results are shown in Table 1-4:

- Baseline with current airport ILS capability (none, Cat I, II, or III)
- The top 100 baseline delay airports with at least Cat I ILS capability
- The top 100 baseline delay airports with at least Cat II ILS capability
- All airports with at least Cat I ILS capability
- All airports with at least Cat II ILS capability

[4] *A Small Aircraft Transportation System (SATS) Demand Model*, Long,Lee,Johnson, and Kostiuk, NASA/CR-2001-210874, June 2001.

Table 1-3. Business Aircraft Results

Total Delay Times in Hours				
	Arrival delay	Departure delay	Delay for planes	Total delay
Base case	598,670	602,372	36,511	1,237,553
Top 100 to Cat I	385,924	420,851	6,609	813,384
Top 100 to Cat II	384,069	418,846	6,431	809,346
All to Cat I	61,604	63,455	5,219	130,278
All to Cat II	46,424	47,681	3,147	97,252
Delay costs and benefits (1999 dollars in millions at $386 per hour of delay)				
	Arrival delay costs	Departure delay costs	Total delay	Total benefits
Base Case	231	233	464	
Top 100 to Cat I	149	162	311	152
Top 100 to Cat II	148	162	310	154
All to Cat I	24	24	48	415
All to Cat II	18	18	36	427

ORGANIZATION OF THE REPORT

Chapters 2–6 document individual airport results. Chapter 7 discusses the noise analysis. Chapter 8 discusses the business aircraft analysis and options for regional aircraft analysis. Chapter 9 contains general conclusions and recommendations for future research. Appendix A describes the models developed for Washington Reagan airport. Appendix B describes the algorithm developed for opposite direction arrivals and departures. Appendix C describes the single runway model. Appendix D discusses the development of dollar values for minutes of delay. Appendix E is a glossary.

Chapter 2
Washington Reagan Airport

General Comments for All Airports

As in the past, we have used the Official Airline Guide (OAG) data to generate airport demand. Specifically this year we used the 1997 OAG.[1] We use the FAA terminal area forecast (TAF) to estimate demand growth for future years. In past efforts we analyzed the OAG data to develop representative days of hourly departure and arrival demand for typical weekdays, and Saturdays and Sundays, for both winter and summer. This year we developed demands for each hour of each day individually. This enabled us to identify information such as individual airline demand, classes of aircraft, and stage lengths on an hour-by-hour basis.

For the current analysis, we used six years of weather data (1990–1995) from the National Weather Service SAMSON II database.

General Comments about Washington Reagan Airport

Washington Reagan airport (DCA) has three intersecting runways, a configuration we have not previously analyzed. We developed new models to address DCA. The new models are described in Appendix A. The runway layout for DCA is shown in Figure 2-1. The wind at DCA is almost evenly split between north and south, as are operations. Washington Reagan has short runways and is operationally constrained by the proximity of restricted areas in the District of Columbia and by man-made and geographic obstacles in Virginia. The Potomac River provides good visual approach paths for both North and South flows, with the North Flow approach being straight to Runway 1.

The demand at Washington Reagan airport is restricted by law, both with respect to the number of operations per hour (60), and the stage length (1,200 miles). Legislation has periodically increased the stage length limit, and recent legislation permits several flights beyond 1,200 miles.

Runway 1/19 is the longest runway with a length of only 6,869 feet. Runway 33/15 is the next longest at 5,189 feet and can support both propeller aircraft and

[1] The 1997 OAG file we used has been processed to remove code-sharing redundancies. Two months, February and December are missing. We used November demand for December and January demand for February. Year 2000 OAG data now are available and will be used for future work.

jets. Runway 3/21 with a length of 4,905 feet and a displaced threshold in the 3 direction, is used for propeller aircraft only. As general policy, propeller aircraft are not offered Runways 1 and 19.

Figure 2-1. Washington Reagan (DCA) Airport Diagram

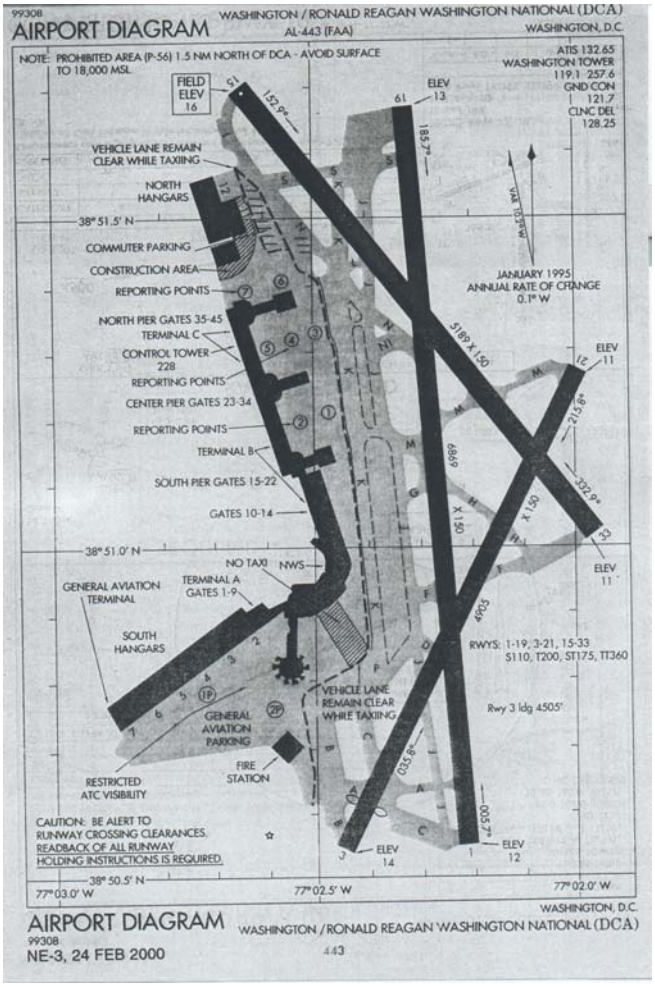

DCA South Flow

The most significant south flow limitation at DCA is the location of the P-56 restricted area that includes the White House, Capitol, Naval Observatory, and much of downtown Washington. The restricted area prevents a straight-in ILS approach to Runway 19. Instead, an unusual LDA, which includes a glideslope, is located so that aircraft descend over Rosslyn, VA and then, visually, make a 40 degree right turn to the runway. Figure 2–2 shows the LDA/DME approach to Runway 19 and the location of the P-56 area.[2] The approach to Runway 21 also is

[2] LDA is localizer-type decision aid, and DME is distance measuring equipment.

obstructed by P-56, and the buildings in Virginia prevent using an ILS with Runway 15. The results of these limitations are minimums for south flow operations of approximately 700 feet ceiling and 2 miles visibility for all runways.

Figure 2-2. DCA Runway 19 LDA/DME Arrival

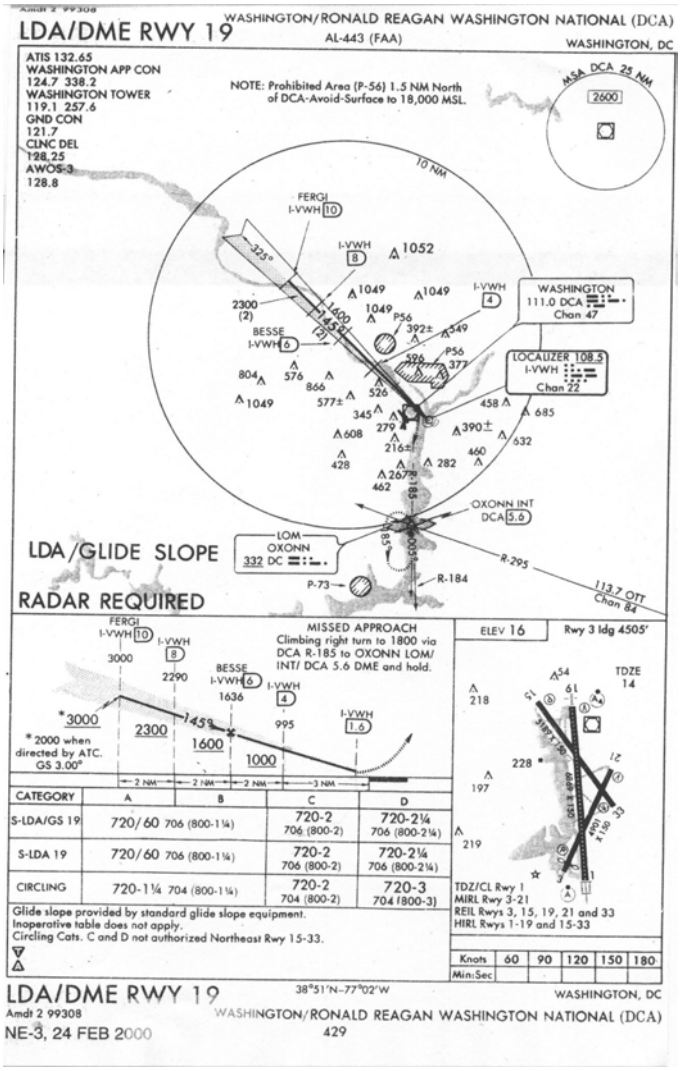

DCA North Flow

As noted above, a clear straight-in approach up the river is possible for Runway 1, and, consequently, Runway 1 is the only ILS-equipped runway. North flow approaches are the only ones available when weather conditions are below 700-2 and only Runway 1 is available when conditions fall below 600-1.5. The Category II minimum for Runway 1 is 150-0.25. When wind conditions favor south flow, but south flow cannot be used because of the low ceiling and visibility, then the north flow will be used with tailwinds. Fully loaded aircraft departing on long flights cannot safely depart downwind on Runway 1, so in tailwind conditions

those aircraft depart upwind directly into the arriving traffic. Such opposite direction arrival-departure operations significantly reduce arrival capacity. Departure capacity is not affected greatly because lighter aircraft can make downwind departures in the long interval between the upwind departure and the subsequent arrival.

The Impact of Synthetic Vision on DCA

Synthetic vision could make all runways available regardless of ceiling and visibility. This capability would allow at least dual-runway arrival capacity in both North and South Flows and would eliminate the need for opposite-direction departure and arrival operations. The benefits are shown in Table 2-1 and graphically in Figure 2–3. Substantially, all the benefits at DCA are achieved with SV1, as shown in Figure 2–2, where the SV1, SV2, and SV3 results are overlain.

Table 2-1. DCA Average Annual Savings (in millions)

Technology	Minutes	1999 constant dollars	1999 present value dollars	Then-year dollars
SV1	0.84	30.8	14.3	41.7
SV2	0.85	31.1	14.4	42.0
SV3	0.87	31.9	14.8	43.1

Figure 2-3. DCA Combined Arrival and Departure Delay versus Technology

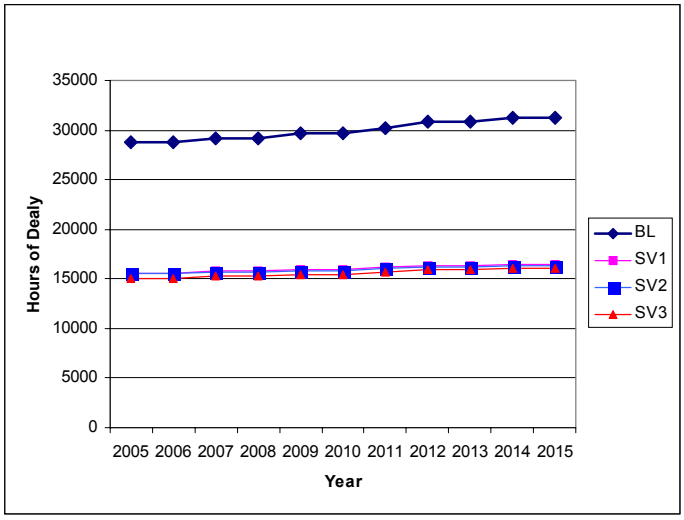

Chapter 3
San Diego Airport (Lindbergh Field)

GENERAL COMMENTS FOR SAN DIEGO

San Diego (SAN) has a single runway, 9/27. Terrain and buildings obstruct the westward approach, Runway 27, which prevents installing a glideslope. Consequently, there is only an LDA approach to Runway 27 with minimums of 660 foot ceiling and 1¾ miles visibility (660-1¾). The eastward approach, Runway 9, has an ILS with minimums of 336 foot ceiling and 5,000 feet visibility (336-1). The runway is 9,400 feet long, but has displaced thresholds in both directions. The prevailing winds favor the Runway 27 approach by 2.5:1. Figure 3-1 shows the runway layout of SAN, and Figure 3-2 shows the Runway 9 ILS approach and the terrain situation.

The demand at SAN was limited in our analysis to the year 2010 level. The FAA TAF predicts a 2010 demand for SAN of 1.35 times the 1997 level. Demands over that amount produce extraordinary delays in our model, and are not likely to be seen in fact.

Figure 3-1. SAN Runway Diagram

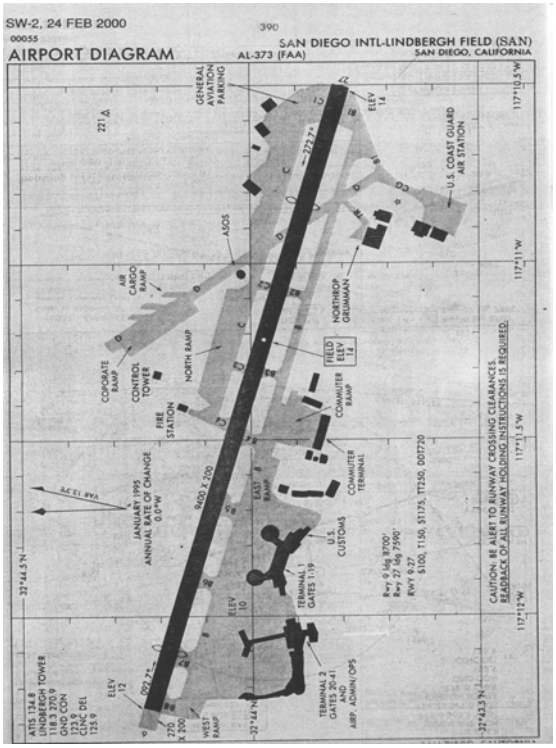

Figure 3-2. SAN Runway 9 ILS Approach

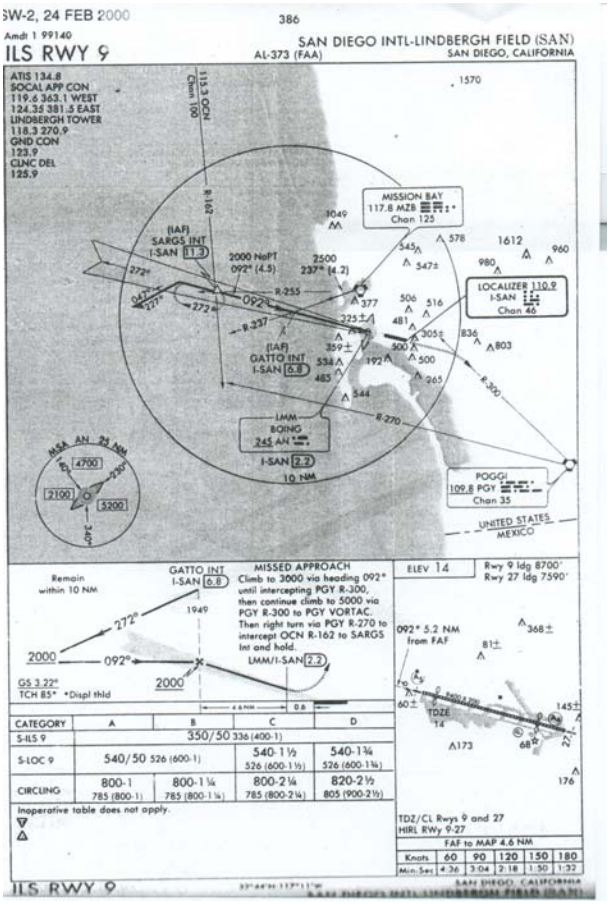

Because missed approaches were reported as a problem at San Diego, we modified the delay model to estimate their impact. We assumed that a missed approach adds an aircraft to the arrival *demand*, and subtracts a departure from the departure *capacity*. In discussions with SAN controller personnel, we found that our assumption is correct. We also found that, contrary to our intuition, missed approaches are a problem in VFR more than in normal IFR. Apparently, unwary aircrews can cut a corner from the visual approach transition point and foul their approach. Missed approaches also are a problem when minimums are near limits for the Runway 9 approach. On one day in May of this year, the ceiling was at the minimum level and the missed approach rate was 50 percent. For baseline operations, we assumed a 5 percent missed approach rate in VFR and a 40 percent missed approach rate when ceilings are within 100 feet of the IFR minimum.

San Diego, like Washington Reagan, is forced to use opposite direction departures and arrivals when minimums require the use of Runway 9 in tailwind conditions.

Impact of Synthetic Vision on SAN

The primary benefits of SV come from lowering the minimums for Runway 27 and eliminating the missed approaches. Lowering the Runway 27 minimums reduces the number of hours the airport closes because conditions are below Runway 27 minimums and Runway 9 has excessive tailwinds. Lowering the minimums also eliminates the opposite-direction departure-arrival operations. The results for SAN are shown in Table 3-1 and Figure 3-3.

Table 3-1. SAN Average Annual Savings (in millions)

Technology	Minutes	1999 constant dollars	1999 present value dollars	Then-year dollars
No Missed Approach	1.21	44.6	19.8	61.2
SV1	1.80	66.0	29.6	90.2
SV2	1.86	68.5	30.7	93.5
SV3	2.03	74.5	33.4	101.8

Figure 3-1. SAN Combined Arrival and Departure Delay versus Technology

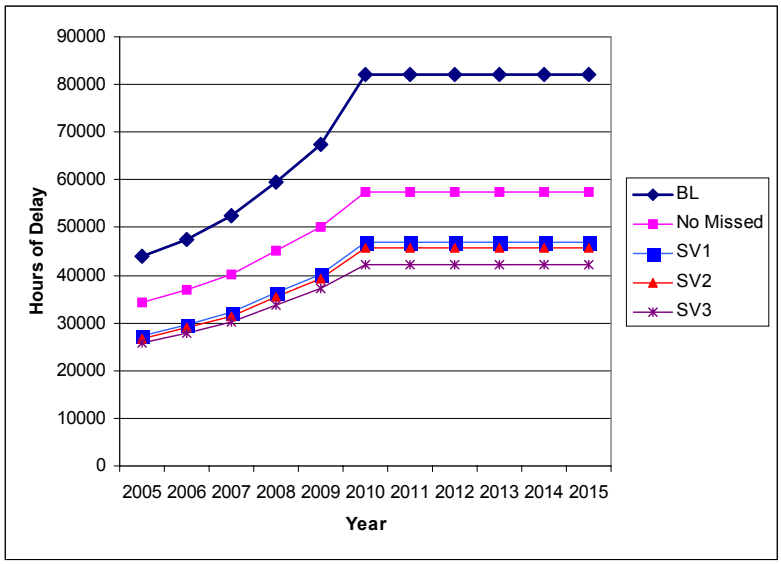

SV benefits San Diego significantly, even when demand is limited to the 2010 expected level. San Diego should be studied more thoroughly in future tasks.

Chapter 4
Juneau Airport

GENERAL COMMENTS FOR JUNEAU

Juneau (JNU) has a single runway, 8/26. The runway is 8,456 feet long and is parallel to a 4,900-foot seaplane water channel. The runway is at sea level and surrounding terrain rises above 4,000 feet. The approach to Runway 26 is through the Gastineau Channel between two rows of mountains. The Runway 8 approach clears 3,000–foot terrain and requires a steep descent to the runway. Neither runway direction can support an ILS because of the terrain. The TERPS LDA-1 approach to Runway 8 has a ceiling minimum of 2,860 feet and a visibility minimum of 4 miles (2860-4). Besides requiring a steep descent, the LDA course is 16 degrees from the runway alignment. There are no instrument approaches to Runway 26 in the TERPS.

The difficulties of JNU have led Alaska Airlines to develop two airline-unique instrument approaches. The first is an LDA approach to Runway 8 with 1000-2 minimums. The second is a set of required navigation performance (RNP) approaches to Runway 26 with minimums ranging from 1260-4 to 337-1 depending on the actual navigation performance (ANP).

Figure 4-1 shows the runway layout for JNU and Figure 4-2 shows the Runway 8 LDA approach and terrain. Figure 4-3 is a nominal RNP approach chart copied from *an Aviation Week & Space Technology* article about RNP.[1]

[1] *RNP Procedures Boost Safety, Ops at Alaska*, Paul Proctor, *Aviation Week & Space Technology*, July 5, 1999, p. 42

Figure 4-1. Juneau Airport Layout

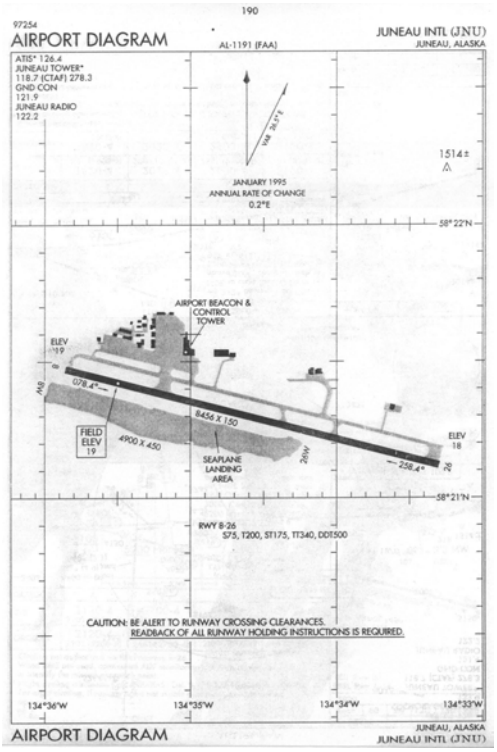

Figure 4-2. Runway 8 LDA Approach

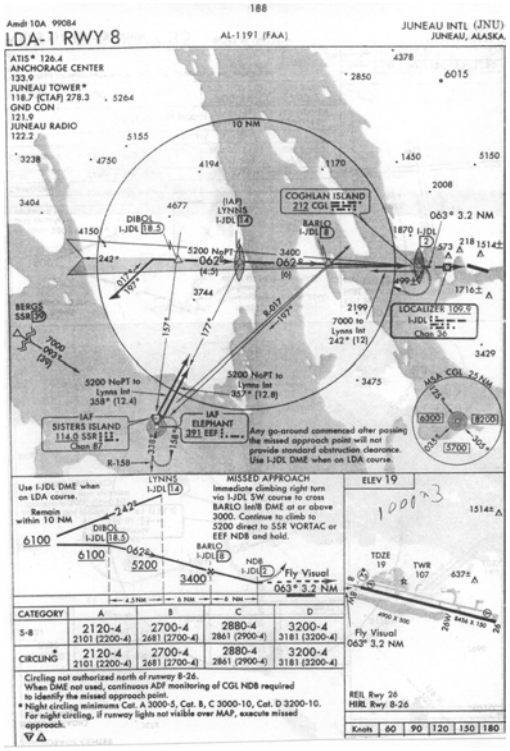

Figure 4-3. Runway 26 RNP

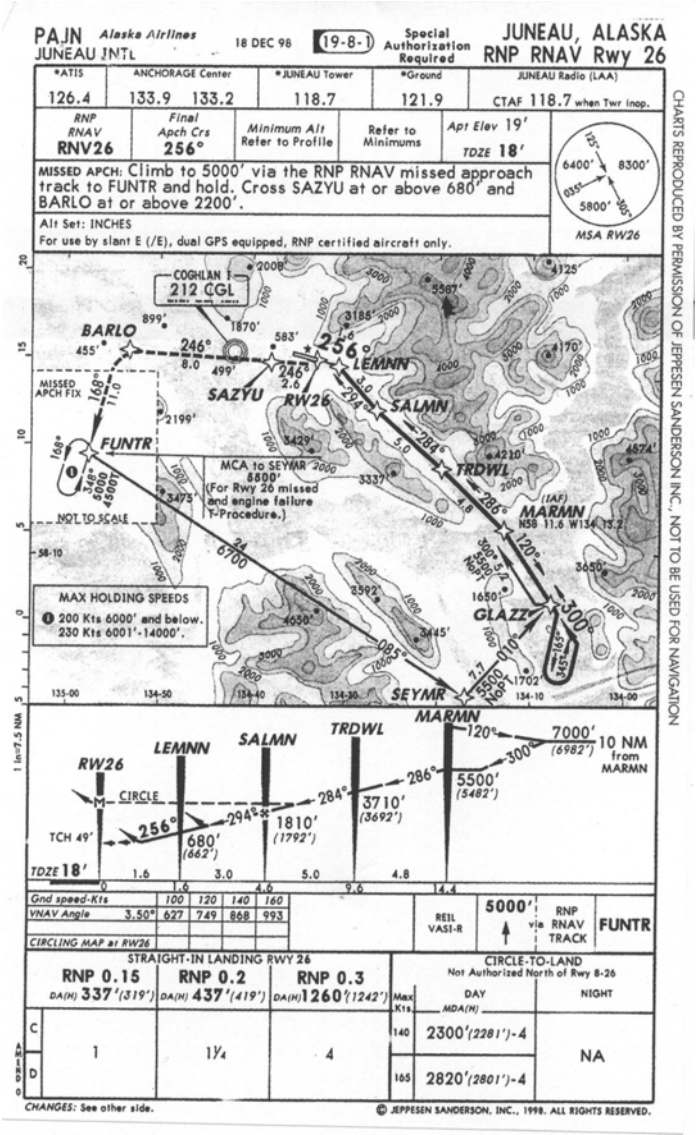

The Impact of Synthetic Vision on JNU

Although SV at Juneau provides benefits similar to RNP, we assume that SV technology will enable reducing minimums further. Selecting the baseline for estimating the benefits at JNU presents an interesting problem. The basic LDA minimums produce such horrendous delays that any major carrier at JNU can logically be expected to have airline-unique LDA procedures such as those developed by Alaska Airlines. Other carriers would not, however, be assumed to have RNP procedures. The majority of carriers at Juneau are VFR air taxi airlines. The TERPS LDA minimums are above the 1000-3 IFR limits, and assuming that air-taxis would still be operating under VFR rules when the airport is below LDA minimums is logical. For both these reasons we believe it is reasonable to assume that the Alaska LDA minimums would be a more appropriate baseline than the

TERPS LDA. Table 4-2 shows the estimated savings for JNU including those for RNP, using the Alaska Airlines LDA as the baseline. Figure 4-2 shows the delay, including that for the TERPS LDA.

Table 4-1. Average Annual Savings (in millions)

Technology	Minutes	1999 constant dollars	1999 present value dollars	Then year dollars
RNP	0.15	5.6	2.6	7.5
SV1	0.21	7.6	3.6	10.3
SV2	0.21	7.7	3.6	10.4
SV3	0.21	7.7	3.6	10.4

Figure 4-4. JNU Combined Arrival and Departure Delay versus Technology

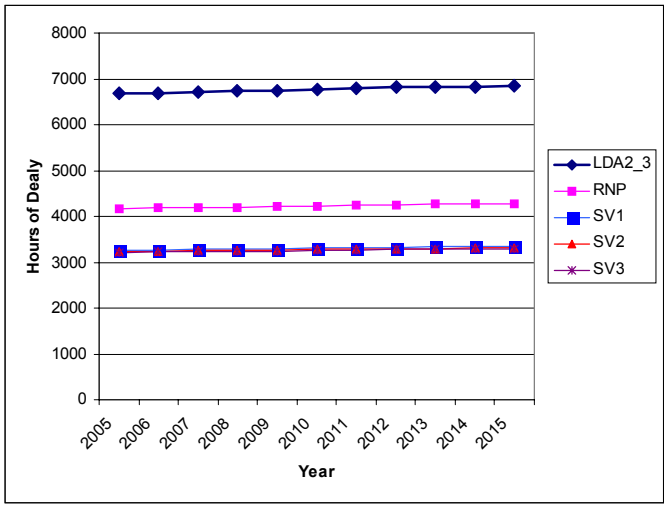

Table 4-2 shows the savings we estimated for Alaska Airlines alone. Figure 4-5 shows the combined arrival and departure delay for the Alaska Airline cases. The current delay model, used with actual schedule data enables us to estimate the delays for specific airlines (see Appendix C). The results are illustrative, but not rigorous, for three reasons. The first reason is assumptions must be made about how many aircraft are originally based at the airport and whether those aircraft can be used to fulfill the current hour's departure demand. The second is that assumptions must be made about how many of the airline's aircraft in the arrival queue are serviced during the hour. The third reason is that discrepancies exist in the OAG between total arrivals and departures that may be due to errors, or may be the result of non-scheduled deadhead or maintenance flights. These issues are discussed in Appendix C.

Table 4-2. Alaska Airlines Average Annual Savings (in Millions)

Technology	Minutes	1999 constant dollars	1999 present value dollars	Then year dollars
RNP	0.035	1.28	0.60	1.73
SV1	0.047	1.74	0.81	2.35
SV2	0.048	1.75	0.82	2.36
SV3	0.048	1.76	0.82	2.37

Figure 4-5. Combined Arrival and Departure Delay for Alaska Airlines at Juneau

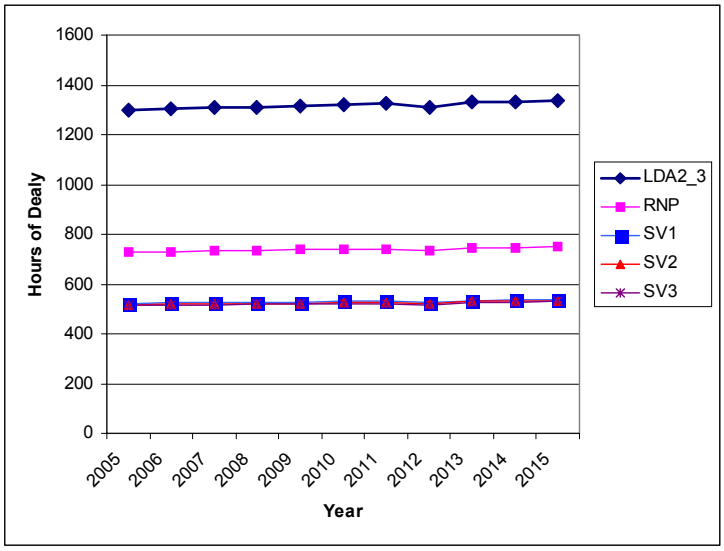

Our analysis, while qualitative, indicates real and reasonable values for SV savings. Juneau presents a surprisingly complex situation with TERPS minimums above the 1000-1 IFR threshold, many VFR-only commercial operations, and at least one carrier with airline-unique, FAA-approved approach procedures. These features could be addressed more directly in future work (see Chapter 9).

Chapter 5
Sacramento International Airport

GENERAL COMMENTS ABOUT SACRAMENTO

Sacramento (SMF) was added to the analysis because it experiences relatively frequent fog conditions. The airport has two widely-spaced parallel 8,600-foot runways, 16 Left and Right and 34 Left and Right. Runways 16R, 16L, and 34L have ILS, and Runway 16R has Cat III capability. In VFR conditions the airport operates with two independent runways, and in heavy fog one runway only one runway is available.

Unfortunately, the SAMSON II weather data for Sacramento are from Sacramento Executive airport (SAC), not the international airport. SMF personnel told us that the weather at the two airports is different, but because of schedule issues and the fact that SAC data does have significant fog, we used the SAC data for the analysis.

Figure 5-1 displays the runway layout for SMF. Unlike the other airports in the study, SMF has no terrain or other unusual features that inhibit arrivals or raise the allowed minimums.

Figure 5-1. Sacramento International (SMF) Airport Diagram

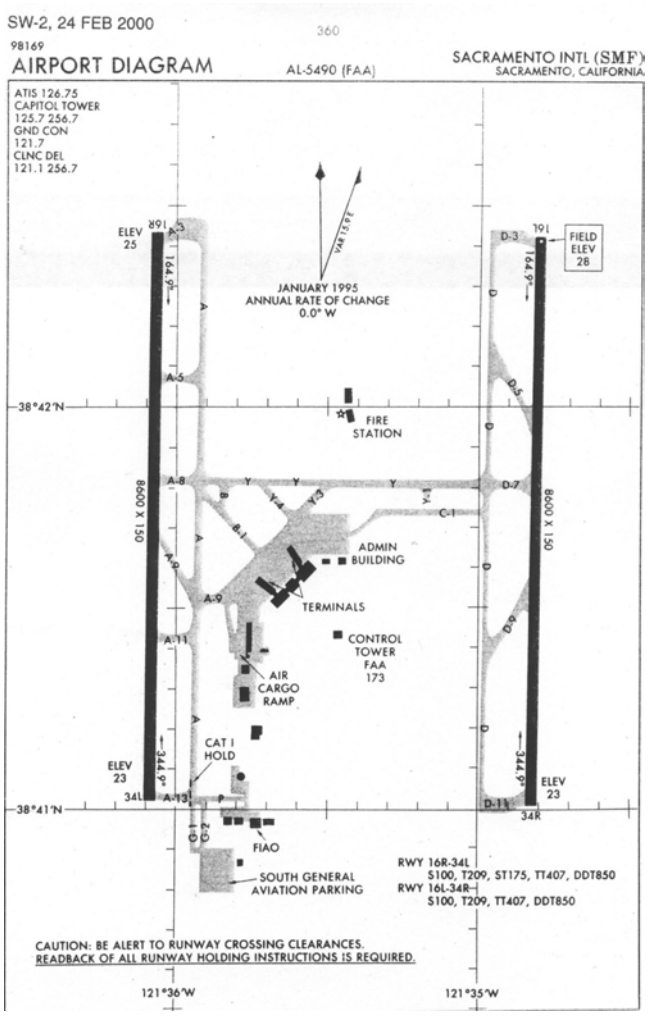

The Impact of Synthetic Vision on SMF

Table 5-1 and Figure 5-2 display the benefits of using synthetic vision at SMF. The savings are not dramatic. The ability to use two runways in both directions at current 600-foot visibility Cat III limits, as provided by SV1, does not reduce delay significantly. Reduction of minimums to 300 feet visibility with SV2 and SV3 is beneficial. Reduction of arrival spacing with SV3 does not provide additional benefit. These results indicate that fog (i.e., visibility > 300 feet and < 600 feet) is the primary problem at SMF and, further, they suggest that SMF is not congested when only OAG air carrier demand is considered. The TAF indicates that adding general aviation (GA) would increase the demand at SMF by about 70 percent, which could very well cause a congestion problem and increase the benefits of SV.

Future work should focus on developing a "schedule" for the GA demand on the basis of tower counts, and on acquiring and using actual SMF weather data.

Table 5-1. SMF Average Annual Savings (in millions)

Technology	Minutes	1999 constant dollars	1999 present-value dollars	Then-year dollars
SV1	0.02	0.64	0.29	0.88
SV2	0.14	5.0	2.3	6.8
SV3	0.14	5.1	2.3	6.9

Figure 5-2. SMF Annual Combined Arrival and Departure Delay

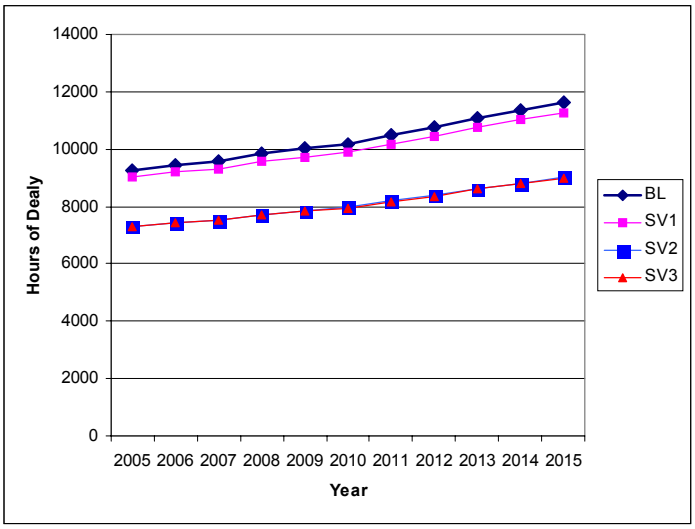

Chapter 6
Eagle County/Vail Airport

GENERAL COMMENTS ABOUT EAGLE/VAIL

Eagle/Vail (EGE) is a single runway airport with an 8,000-foot runway. The salient features of EGE are its 6,535-foot elevation and the surrounding mountains that rise as high as 14,000 feet. There are no ILS approaches and the lowest minimums are provided by a GPS approach with limits of 2,245-foot ceiling and 3-mile visibility. Departure minimums are a 700-foot ceiling and 2-mile visibility given a minimum climb capability of 480 (Runway 7) or 750 (Runway 25) feet/nautical mile. Figure 6-1 shows the GPS approach to EGE and the surrounding terrain. We used the best current minimums for the baseline.

Figure 6-1. EGE GPS-D Approach

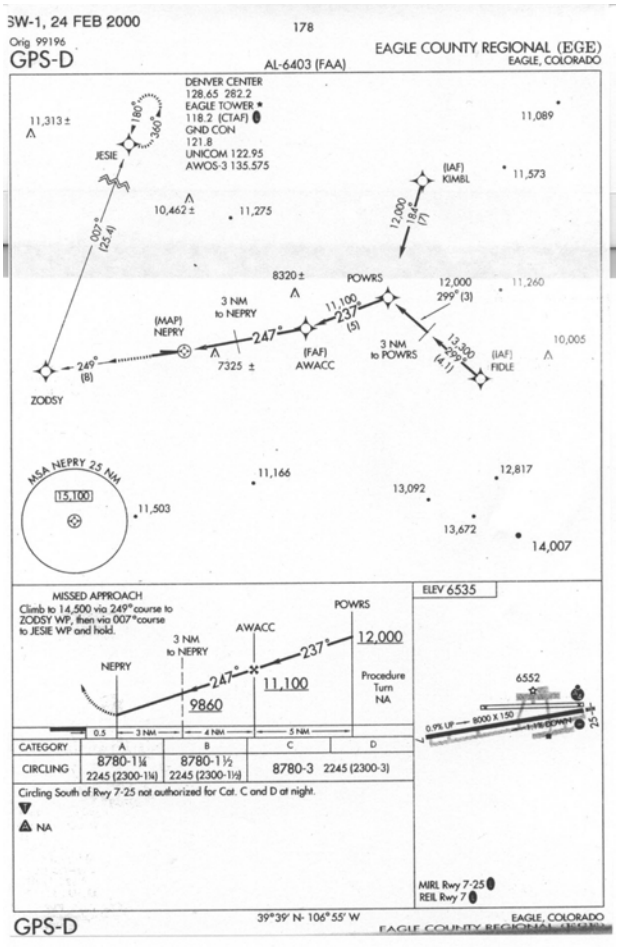

The scheduled demand at EGE is small. The OAG only shows one arrival flight per day, a B757, during most of the year. Queries on Travelocity™ showed the B757, a few commuter aircraft, and a bus; moreover, for year 2005, the TAF predicts only 35,000 total operations for EGE including GA and military. With demand so low, normal delay-based benefit analysis would be fruitless. In light of this, we decided that constructing an artificial demand of one arrival per hour with a departure the next hour to see what the expected delay would be as a function of month and hour of day might be more useful. In this model, an arrival is delayed if the weather is below airport minimums and is assumed to land with no delay if weather is above minimums, i.e., capacity is assumed infinite when the airport is open and zero when closed. A departure can be delayed by weather, or by lack of an aircraft, or by both.

The analysis produces tables of minutes of delay in arrival or departure for a given hour of a given month. The number represents the amount of delay expected if one was scheduled to arrive (or depart) at a certain hour (e.g., 0800) in a certain month (e.g., February). Originally, we averaged the delay over all hours, but then found it more informative to calculate the "conditional" delay that occurs if weather for the hour is bad. A separate table contains the averaged number of bad hours per month for the given hour and month. Tables 6-1 through 6-4 contain the baseline conditional delays and bad-hour frequencies, and Figure 6-2 is a graphical display of the baseline conditional arrival table (Table 6-1) data.

Table 6-1. EGE Baseline Conditional Arrival Delay

Month	Hour																							
	1	2	3	4	5	6	7	8	9	10	11	12	13	14	15	16	17	18	19	20	21	22	23	24
Jan	73	63	86	59	56	49	51	74	74	121	155	116	167	167	149	131	109	77	68	62	94	85	85	73
Feb	127	159	115	98	123	126	127	109	87	129	113	162	92	139	82	103	62	156	122	117	110	151	128	120
Mar	128	203	125	90	84	76	68	65	55	58	87	106	67	57	77	91	93	90	92	101	139	112	111	136
Apr	69	59	83	58	98	80	96	113	181	99	88	136	121	61	73	64	54	51	51	46	43	60	74	65
May	144	129	118	70	77	60	46	34	33	18	50	50	81	58	39	56	54	67	56	46	56	169	159	140
Jun	56	43	34	51	43	43	36	24	13	0	0	0	0	9	0	0	16	9	34	26	13	16	0	17
Jul	0	34	51	39	26	34	29	13	0	0	0	0	9	17	9	9	0	9	0	0	0	0	0	0
Aug	9	0	0	50	47	50	31	24	16	9	0	0	0	0	13	9	0	0	0	0	0	9	0	17
Sep	47	36	36	32	23	28	27	20	31	39	136	74	77	94	91	108	141	95	65	103	96	76	66	60
Oct	71	69	53	69	54	35	29	19	52	70	52	53	65	56	40	30	17	11	0	9	0	54	43	34
Nov	114	108	95	90	74	53	59	34	54	46	54	54	52	61	46	48	67	75	90	165	189	159	155	161
Dec	130	109	107	97	81	77	49	40	48	69	267	200	194	140	125	186	232	160	201	115	124	150	129	136

Table 6-2. EGE Baseline Conditional Departure Delay

Month	Hour of Day																							
	1	2	3	4	5	6	7	8	9	10	11	12	13	14	15	16	17	18	19	20	21	22	23	24
Jan	30	42	53	41	31	43	31	64	44	65	80	59	72	67	61	52	47	37	38	28	30	39	43	33
Feb	113	137	93	91	110	98	158	87	128	87	69	110	104	113	102	102	84	45	84	84	121	111	80	97
Mar	119	201	180	85	102	72	70	62	55	61	97	73	74	43	55	81	42	86	56	46	112	79	99	117
Apr	49	44	51	59	106	84	48	121	194	101	95	141	131	111	103	67	53	48	44	42	48	61	41	30
May	89	113	98	106	66	82	53	51	38	29	21	27	17	23	31	17	13	21	27	21	24	23	99	91
Jun	9	9	9	9	26	34	35	22	21	0	0	0	0	9	0	0	9	0	0	9	9	9	0	0
Jul	0	0	9	13	13	16	21	21	0	0	0	0	9	0	9	9	0	0	0	0	0	0	0	0
Aug	9	0	0	9	27	35	38	54	23	9	0	0	0	0	9	9	0	0	0	0	0	0	0	0
Sep	34	32	29	40	32	36	29	34	43	64	43	80	54	56	56	54	76	69	47	59	54	50	38	34
Oct	9	13	16	18	46	38	28	33	34	34	46	17	14	11	13	13	9	9	0	0	0	9	13	9
Nov	65	99	97	81	63	65	107	35	125	42	54	29	27	28	24	31	54	63	65	54	142	116	99	121
Dec	83	93	76	68	67	73	50	28	59	57	42	125	121	125	90	127	132	112	118	92	107	125	112	93

Table 6-3. EGE Baseline Frequency of Hours Below Arrival Minimums

Month	Hour																							
	1	2	3	4	5	6	7	8	9	10	11	12	13	14	15	16	17	18	19	20	21	22	23	24
Jan	2.9	2.4	2.1	2.1	2.4	2.1	3.4	2.6	2.4	3	1.7	1.4	1.3	1.4	1.3	1.4	1.6	1.7	1.3	1.7	2.3	2.4	2	2.6
Feb	3.1	2.6	3.1	3	1.7	2.3	1.9	1.9	2.1	1.4	1.3	1.1	1.4	1.1	1	0.9	1.1	1.3	1.7	2	2.4	2	2.6	2.9
Mar	2.4	1.9	3.3	3.4	4.3	3.4	3.3	3.1	2.7	2	2	1.6	1.3	1.3	2.3	1.3	1.4	2	2.6	3	2.6	4	3.9	3.1
Apr	2.1	1.9	1.9	2	1.7	1.6	2.3	2	1.1	1	1.1	1	1.1	1	0.6	0.7	0.6	0.7	0.9	1.6	1	0.9	1.4	1.4
May	0.9	1.3	1.6	1.4	1.6	1.7	1.6	1.4	1.3	0.9	0.6	0.6	0.3	0.9	0.6	0.3	0.6	0.9	0.9	0.9	0.7	1	0.9	0.9
Jun	0.4	0.3	0.4	0.6	0.9	1	1.3	1	0.4	0	0	0	0	0.1	0	0	0.4	0.1	0.1	0.1	0.3	0.6	0	0.3
Jul	0.1	0.3	0.3	0.3	0.3	0.7	0.4	0.3	0	0	0	0	0.1	0.1	0.1	0.1	0	0.1	0	0.1	0	0.1	0.1	0.3
Aug	0.4	0.1	0.3	1	1.6	2	2.1	1.1	0.7	0.1	0	0	0	0	0.3	0.1	0	0	0	0	0	0.1	0	0.1
Sep	1.1	1.1	1	0.9	0.9	1	1.1	1.3	0.6	0.3	0.4	0.6	0.6	0.6	0.6	0.6	0.6	0.7	0.9	0.6	0.4	0.7	1	1.1
Oct	1	1.1	1	1.3	2	2.4	2.3	2.4	1.6	1.6	1.1	1	0.7	0.7	1	0.9	0.6	0.6	0.1	0.3	0.3	0.7	0.7	1
Nov	2.4	2.3	2.3	2.4	2.6	2.9	2.7	2.6	1.7	1.6	1.1	0.9	0.9	1	1.1	2	1	1.1	0.9	1.7	1.4	1.3	1.9	1.6
Dec	3.9	3.3	3.1	3.1	3.4	3.9	3.7	3.1	2.6	2	1.6	2	2	1.9	1.9	1.6	1.9	2.7	2.9	3.4	3	2.4	3.1	3.1

Table 6-4. EGE Baseline Frequency of Hours Below Departure Minimums

Month	Hour																							
	1	2	3	4	5	6	7	8	9	10	11	12	13	14	15	16	17	18	19	20	21	22	23	24
Jan	2.3	2.3	1.3	1.7	2	1.7	2.3	2.1	2	2.1	1.6	1.1	1	1.3	1.3	1.1	1	1.4	1	1.4	1.6	2	1.6	1.6
Feb	2.4	2.6	2.3	2.1	1.4	1.4	1.6	1.6	1.3	1.1	1	1.1	1	1	0.7	0.6	0.7	1	1	1.7	2	1.4	1.6	2
Mar	2.3	1.7	2	3.1	3.1	2.7	2.9	2.7	2.3	1.9	1.9	1.3	1	0.9	1.3	1	1	1	1.7	2.6	2.1	3.1	3.6	2.6
Apr	1.1	1.7	1.3	1.4	1.1	1.3	1.7	1.7	0.9	0.7	1	0.6	0.9	0.6	0.4	0.4	0.6	0.6	0.9	0.9	0.9	0.6	0.6	1.1
May	0.6	1	1.1	1.1	1.3	1.3	1.3	1.3	1.1	0.9	0.3	0.4	0.1	0.7	0.6	0.1	0.3	0.6	0.7	0.7	0.6	0.4	0.7	0.7
Jun	0.3	0.3	0.3	0.4	0.7	0.7	0.9	0.9	0.4	0	0	0	0	0.1	0	0	0.1	0	0	0.1	0.1	0.1	0	0.1
Jul	0.1	0	0.1	0.3	0.3	0.4	0.4	0.3	0	0	0	0	0.1	0	0.1	0.1	0	0	0	0	0	0	0.1	0.3
Aug	0.1	0.1	0.1	0.6	1.3	1.6	1.7	1	0.7	0.1	0	0	0	0	0.1	0.1	0	0	0	0	0	0	0	0
Sep	1	1	0.9	0.7	0.7	0.9	1	1.1	0.6	0.3	0.1	0.4	0.4	0.6	0.6	0.4	0.4	0.6	0.7	0.4	0.4	0.4	0.7	0.7
Oct	0.6	0.9	0.9	0.9	1.1	1.7	1.6	2	1.1	1.4	1.1	0.7	0.6	0.6	0.7	0.7	0.6	0.4	0.1	0.1	0.1	0.4	0.6	0.9
Nov	1.7	2	1.6	1.6	2.3	2.4	2.1	2.6	1	1.6	0.6	0.9	0.7	0.6	0.7	0.7	1	0.7	0.9	1.1	1	1.1	1.3	1.4
Dec	2.7	3	2.4	2.9	3	2.9	3.1	2.7	1.7	1.4	1.4	0.9	1.6	1.6	1.6	1.3	1.6	2.1	2.6	3	2.9	2.1	2.1	2.7

Figure 6-2. EGE Baseline Conditional Arrival Delay

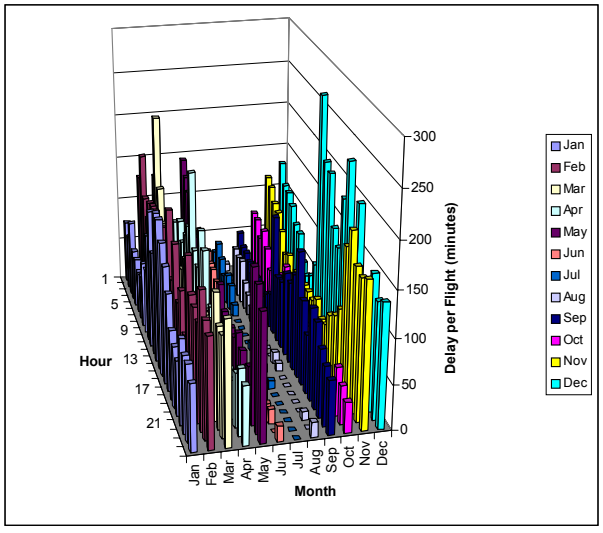

The data in the preceding tables indicate significant delay problems at EGE. With SV1, the arrival minimums are reduced to Cat III levels: 0-foot ceiling and 600-foot visibility. Departure minimums similarly are reduced to 700 feet of visibility. These reductions essentially eliminate delays as shown in Tables 6-5 through 6-8 and Figure 6-3 below.

Table 6-5. EGE SV1 Conditional Arrival Delay

Month	Hour																							
	1	2	3	4	5	6	7	8	9	10	11	12	13	14	15	16	17	18	19	20	21	22	23	24
Jan	0	0	0	0	0	0	0	0	0	0	0	0	0	0	0	0	0	0	0	0	0	0	0	0
Feb	0	0	0	0	0	0	0	17	9	0	0	0	0	0	0	0	0	0	0	0	9	0	0	0
Mar	0	0	0	0	17	9	0	0	0	0	0	0	0	0	0	0	0	0	9	0	0	9	0	0
Apr	0	9	0	0	0	0	0	9	0	0	17	9	0	0	0	0	0	0	0	0	0	0	0	0
May	0	0	0	0	0	26	17	9	0	0	0	0	0	21	9	0	0	0	0	0	0	0	0	0
Jun	0	0	0	0	0	0	0	0	0	0	0	0	0	9	0	0	9	0	0	0	0	0	0	0
Jul	0	0	0	0	0	0	0	0	0	0	0	0	9	0	0	9	0	0	0	0	0	0	0	0
Aug	0	0	0	9	0	0	0	0	0	0	0	0	0	0	9	9	0	0	0	0	0	0	0	0
Sep	0	0	9	0	9	0	17	9	0	0	0	9	0	9	9	0	0	0	0	0	0	0	0	9
Oct	0	0	0	0	0	0	17	13	0	0	0	0	0	0	0	0	0	0	0	0	0	0	0	0
Nov	0	0	0	0	0	0	0	0	0	0	0	0	0	0	0	0	0	0	0	0	0	0	0	0
Dec	0	0	0	0	0	0	17	21	9	0	0	0	0	0	0	0	0	0	0	0	0	0	0	0

Table 6-6. EGE SV1 Conditional Departure Delay

Month	Hours																							
	1	2	3	4	5	6	7	8	9	10	11	12	13	14	15	16	17	18	19	20	21	22	23	24
Jan	0	0	0	0	0	0	0	0	0	0	0	0	0	0	0	0	0	0	0	0	0	0	0	0
Feb	0	0	0	0	0	0	0	9	26	0	0	0	0	0	0	0	0	0	0	0	0	0	0	0
Mar	0	0	0	0	0	9	0	0	0	0	0	0	0	0	0	0	0	0	0	0	0	0	0	0
Apr	0	0	0	0	0	0	0	9	0	0	9	17	0	0	0	0	0	0	0	0	0	0	0	0
May	0	0	0	0	0	9	26	26	0	0	0	0	0	13	26	0	0	0	0	0	0	0	0	0
Jun	0	0	0	0	0	0	0	0	0	0	0	0	0	9	0	0	9	0	0	0	0	0	0	0
Jul	0	0	0	0	0	0	0	0	0	0	0	0	9	0	0	9	0	0	0	0	0	0	0	0
Aug	0	0	0	9	0	0	0	0	0	0	0	0	0	0	9	9	0	0	0	0	0	0	0	0
Sep	0	0	0	0	0	0	0	9	0	0	0	9	0	9	17	0	0	0	0	0	0	0	0	0
Oct	0	0	0	0	0	0	9	26	0	0	0	0	0	0	0	0	0	0	0	0	0	0	0	0
Nov	0	0	0	0	0	0	0	0	0	0	0	0	0	0	0	0	0	0	0	0	0	0	0	0
Dec	0	0	0	0	0	0	0	13	26	0	0	0	0	0	0	0	0	0	0	0	0	0	0	0

Table 6-7. EGE SV1 Frequency of Hours Below Arrival Minimums

Month	Hour																							
	1	2	3	4	5	6	7	8	9	10	11	12	13	14	15	16	17	18	19	20	21	22	23	24
Jan	0	0	0	0	0	0	0	0	0.1	0.1	0.1	0	0	0	0	0	0	0	0	0	0	0	0	0
Feb	0	0	0	0	0	0	0	0.1	0.1	0	0	0	0	0	0	0	0	0	0	0	0.1	0	0	0
Mar	0	0	0	0	0.1	0.1	0	0	0	0	0	0	0	0	0	0	0	0	0.1	0	0	0.1	0	0
Apr	0	0.1	0	0	0	0	0	0.1	0	0	0.1	0.1	0	0	0	0	0	0	0	0	0	0	0	0
May	0	0	0	0	0	0.1	0.1	0.1	0	0	0	0	0	0.3	0.1	0	0	0	0	0	0	0	0	0
Jun	0	0	0	0	0	0	0	0	0	0	0	0	0	0.1	0	0	0.1	0	0	0	0	0	0	0
Jul	0	0	0	0	0	0	0	0	0	0	0	0	0.1	0	0	0.1	0	0	0	0	0	0	0	0
Aug	0	0	0	0.1	0	0	0	0	0	0	0	0	0	0	0.1	0.1	0	0	0	0	0	0	0	0
Sep	0	0	0.1	0	0.1	0	0.3	0.3	0	0	0	0.1	0	0.1	0.1	0	0	0	0	0	0	0	0	0.1
Oct	0	0	0	0	0.1	0	0.1	0.3	0	0	0	0	0	0	0	0	0	0	0	0	0	0	0	0
Nov	0	0	0	0	0	0.1	0	0	0	0	0	0	0	0	0	0	0	0	0	0	0	0	0	0
Dec	0	0	0	0	0	0.1	0.3	0.3	0.1	0	0	0	0	0	0	0	0	0	0	0	0	0	0	0

Table 6-8. EGE Baseline Frequency of Hours Below Departure Minimums

Month	Hours																							
	1	2	3	4	5	6	7	8	9	10	11	12	13	14	15	16	17	18	19	20	21	22	23	24
Jan	0	0	0	0	0	0	0	0	0.1	0.1	0	0	0	0	0	0	0	0	0	0	0	0	0	0
Feb	0	0	0	0	0	0	0	0.1	0.1	0	0	0	0	0	0	0	0	0	0	0	0	0	0	0
Mar	0	0	0	0	0	0.1	0	0	0	0	0	0	0	0	0	0	0	0	0	0	0	0	0	0
Apr	0	0	0	0	0	0	0	0.1	0	0	0.1	0.1	0	0	0	0	0	0	0	0	0	0	0	0
May	0	0	0	0	0	0.1	0.1	0.1	0	0	0	0	0	0.3	0.1	0	0	0	0	0	0	0	0	0
Jun	0	0	0	0	0	0	0	0	0	0	0	0	0	0.1	0	0	0.1	0	0	0	0	0	0	0
Jul	0	0	0	0	0	0	0	0	0	0	0	0	0.1	0	0	0.1	0	0	0	0	0	0	0	0
Aug	0	0	0	0.1	0	0	0	0	0	0	0	0	0	0	0.1	0.1	0	0	0	0	0	0	0	0
Sep	0	0	0	0	0	0	0	0.3	0	0	0	0.1	0	0.1	0.1	0	0	0	0	0	0	0	0	0
Oct	0	0	0	0	0	0	0.1	0.1	0	0	0	0	0	0	0	0	0	0	0	0	0	0	0	0
Nov	0	0	0	0	0	0	0	0	0	0	0	0	0	0	0	0	0	0	0	0	0	0	0	0
Dec	0	0	0	0	0	0	0.1	0.3	0.1	0	0	0	0	0	0	0	0	0	0	0	0	0	0	0

Figure 6-3. EGE SV1 Conditional Arrival Delay

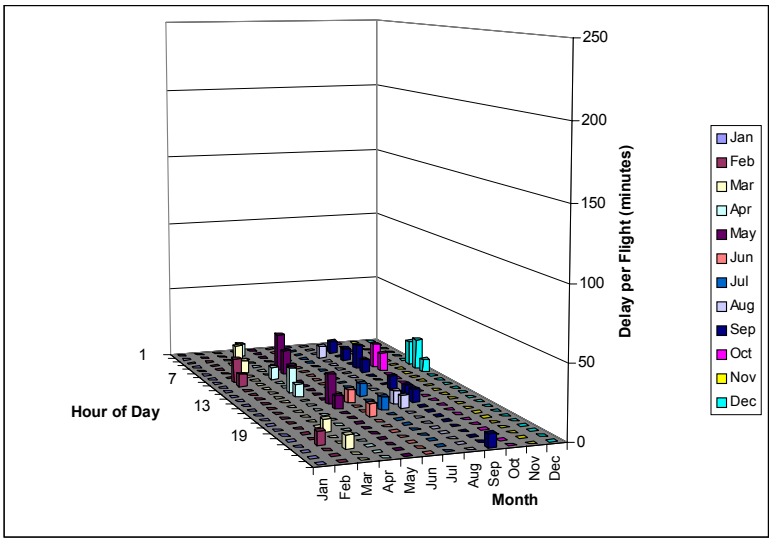

The foregoing analysis indicates dramatic benefits at EGE. Our analysis is based on the assumption that weather conditions prevail for the entire hour they are reported, and that the large baseline delays are due to contiguous hours of weather below minimums. Future work should investigate whether the airport is truly shut down for periods of hours or whether flights can arrive and depart during periods of clearing. Varying the minimums in the model to determine the highest minimums that will result in significant delay reductions is also recommended for future work.

Chapter 7
Noise Analysis

Noise reduction has been proposed as a potential indirect benefit of SV technology. The benefit is based on the ability to use low-noise flight tracks in all weather conditions. In the current task, we used the ASAC noise model of Washington Reagan airport to determine if increased use of the VFR river routes would reduce noise exposure at DCA.

The ASAC noise model is based on the FAA Integrated Noise Model (INM). Inputs include the flight tracks and demand and equipment types for the airport. Outputs include 24-hour average noise contours; estimates of the population, residences and businesses; and physical area contained in each noise contour.

We ran two cases. In the first, we compared the noise footprint from 100 percent use of VFR river routes to the airport baseline, which includes VFR and IFR routes. In the second, we compared 100 percent VFR river routes to the noise footprints from the DCA IFR routes. Table 7-1 shows the population results from the analysis. Figures 7-1 and 7-2 display the contour maps of the results.

Table 7-1. DCA Noise Analysis Result

Sound Level	River Routes	All Conditions		IFR Conditions	
(dB)	Population	Population	Difference (%)	Population	Difference (%)
75	1,327	1,335	-0.60	1,406	-5.62
70	6,508	6,509	-0.02	6,000	8.47
65	33,999	34,013	-0.04	34,640	-1.85
60	102,975	103,428	-0.44	115,087	-10.52
55	246,526	247,899	-0.55	269,506	-8.53

Figure 7-1. Baseline and 100-Percent VFR River-Route Noise-Contour Maps

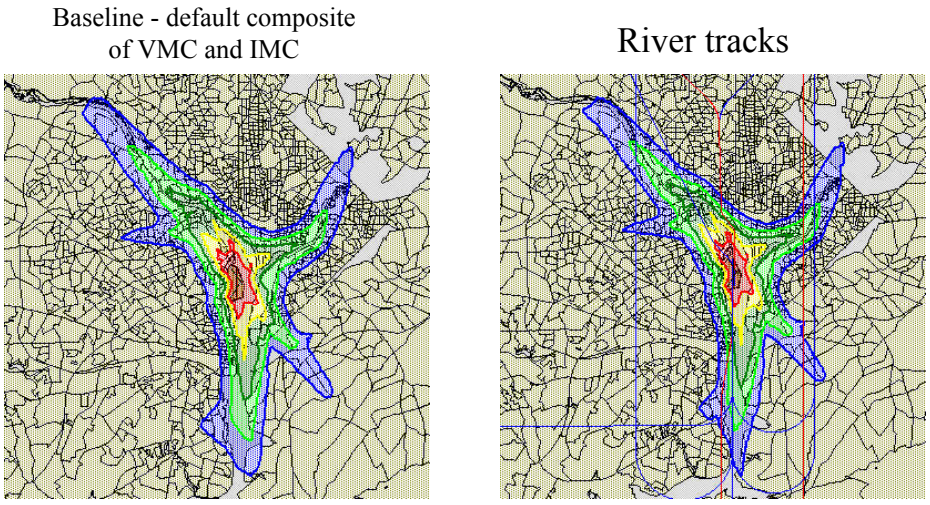

Figure 7-2. All ILS and 100-Percent VFR River-Route Noise-Contour Maps

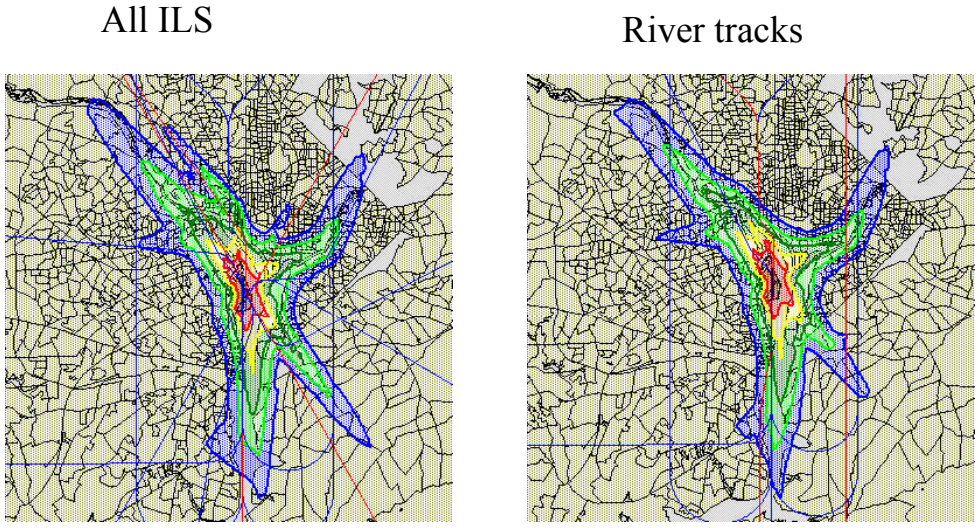

The noise improvement is modest. This is because the current IFR routes are not much different than the VFR river routes. Although we do not recommend further noise analysis of DCA, SV may benefit other airports. Table 7-3 lists the airports for which we have ASAC noise models. Because the models are available, a survey of the potential SV benefits at the airports listed in the table would be a useful element of future work.

Table 7-2. Existing ASAC Airport Noise Models

Adelaide Australia	Los Angeles (LAX)	Seattle-Tacoma (SEA)
Atlanta (ATL)	Minneapolis (MSP)	Washington Dullas (IAD)
Boston (BOS)	New York Kennedy (JFK)	Zurich, Switzerland
Chicago (ORD)	New York Laguardia (LGA)	Cleveland (CLE)
Cincinnati (CVG)	Newark (EWR)	Baltimore-Washington (BWI)
Dallas-Ft Worth (DFW)	Orlando (MCO)	Washington Reagan (DCA)
Detroit (DTW)	Pittsburgh (PIT)	Williamsburg (PHF)
Frankfurt, Germany	San Francisco (SFO)	Norfolk (NOR)

Chapter 8
Benefits of SV for Business and Regional Aircraft

We estimated the benefits of SV to business aircraft by using information developed in analyses of the NASA Small Aircraft Transportation System (SATS). For the SATS analysis, we developed a network of 2,865 airports and a corresponding demand scenario for use with our LMINET model.[1] The locations of the SATS airports are shown in Figure 8-1. For this task, we determined annual arrival delays and departure delays using a modified version of LMINET that neglects congestion effects and treats each airport as either open or closed. An airport was open if meteorological conditions were better than the airport's present IFR ceiling and visibility minimums, closed if not. We considered only twin turboprop aircraft in this analysis.

Figure 8-1. SATS Airports

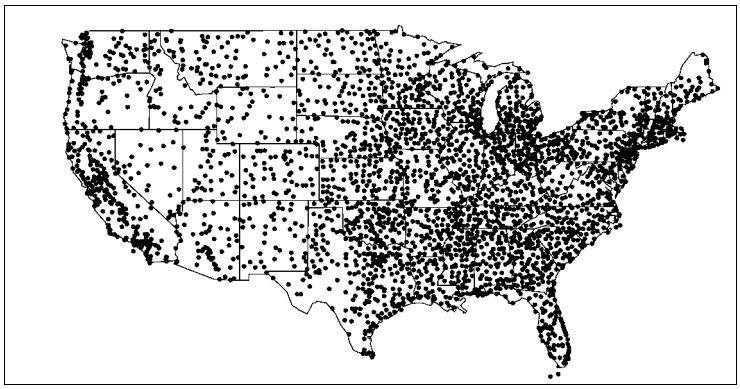

Unlike past LMINET analyses, which used a few selected days of weather, our current analysis uses the complete weather for 1995. The weather data were taken from the National Weather Service SAMSON II database which includes weather for 262 continental United States weather stations (mostly at airports). Figure 8-2 shows the locations of the SAMSON II weather stations. We mapped the 262 weather stations by hand to the 2,865 SATS airports according to location and geographical considerations.

[1] *A Small Aircraft Transportations System (SATS) Demand Model*, Long, Lee, Johnson, and Kostiuk, NASA/CR-2001-210874, June 2001.

Figure 8-2. SAMSON II Weather Station Locations

We determined the existence and type of ILS capabilities at the SATS airports from two sources. We downloaded information about Category 1 ILS airports from an unofficial Internet site, http://www.fallinggrain.com/air/cache/geo/USGA/ILS.html. Our attempts to transfer official Category 1 ILS data from the FAA failed twice, but we will try again in future work. We obtained data for Category 2 and 3 airports from the FAA AFS-410 Flight Operations Branch web-site at, http://www.faa.gov.avr/afs/afs410/afs410.htm.

We ran the model with baseline capabilities. Figure 8-3 shows the locations of the 100 airports with the highest totals of delays for arrivals and departures in this scenario. As one would expect, none of the airports had ILS. Changing their capabilities to ILS Category I significantly reduced delay totals. Further improvement to ILS Category II gave only minimally improved delays because Category II weather conditions occur much less frequently than Category I.

Figure 8-3. Top 100 SATS Business Delay Airports

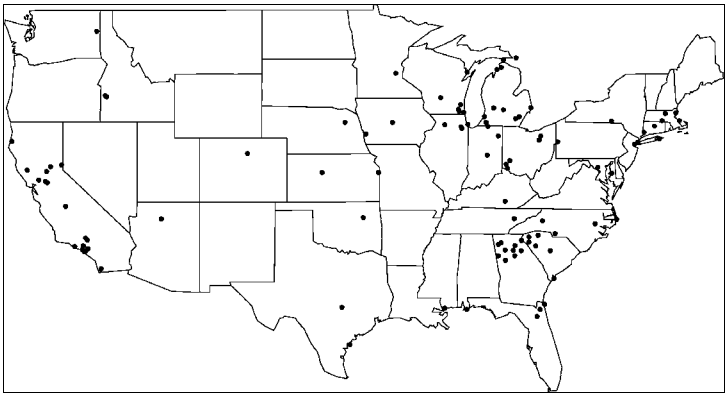

We then accumulated delay totals with the capabilities of all of the 2,865 SATS airports changed. We first changed the airports' minimums to the better of ILS Category I and the airports' present capabilities, and then to the better of ILS Category II and their present capabilities. Total delays, although much lower than those found in the first three cases, told a similar story. The change to ILS Cate

gory I reduced delays substantially, while the change to ILS Category II gave only modest further improvement. Table 8-1 summarizes our delay results.

Table 8-1.Total Delay Times for Business Aircraft (in hours)

	Arrival delay	Departure delay	Delay for planes	Total delay
Base Case	598,670	602,372	36,511	1,237,553
Top 100 to Cat I	385,924	420,851	6,609	813,384
Top 100 to Cat II	384,069	418,846	6,431	809,346
All to Cat I	61,604	63,455	5,219	130,278
All to Cat II	46,424	47,681	3,147	97,252

We also investigated the dollar values of these possible changes. Ground delay is the appropriate cost measure, because carriers take delays for closed destination airports on the ground at the departure airport. By averaging the direct operating costs for a 16-passenger aircraft, we determined that $386 in FY 1999 dollars is a reasonable value for the cost of one hour of ground delay.

Applying this figure to the delay totals of Table 8-1, we find the greatest cost, $464 million, reflecting annual cost of arrival and departure delays with original SATS airport capabilities. A cost of $311 million results when the 100 worst airports are changed to ILS Category I, and $310 million when they are changed to ILS Category II. Lower figures of $48 million and $36 million reflect changing all airports to ILS Category I and to ILS Category II, respectively. Table 8-2 summarizes these results.

Table 8-2.Total Delay Costs and Benefits for Business Aircraft (in millions)

	Arrival delay cost (dollars)	Departure delay cost (dollars)	Total delay cost (dollars)	Total benefits (dollars)
Base Case	231	233	464	
Top 100 to Cat I	149	162	311	152
Top 100 to Cat II	148	162	310	154
All to Cat I	24	24	48	415
All to Cat II	18	18	36	427
Note: Delay costs and benefits are calculated using 386 costant 1999 dollars per hour of delay.				

Regional Aircraft Benefits

We have gathered initial information from the OAG data on regional schedules for specific airlines and airports, but have not completed the detailed demand itineraries needed for LMINET analysis. A brief manual review of the regional aircraft data indicates that essentially all regional operations are to airports that currently have ILS or GPS approaches, so economic benefits are not expected to be as dramatic as the business aircraft results.

We recommend developing specific regional demand schedules and a corresponding LMINET analysis for future work.

Chapter 9
Conclusions and Recommendations

CONCLUSIONS

Individual Airport Benefits. The individual airport results for Washington Reagan, San Diego, and Juneau indicate significant potential economic benefits from using SV technology. Our underlying assumptions are that SV can enable safe use of curved IFR and reduced minimums at airports currently limited by natural or man-made obstructions. Significant benefits have already been achieved at Juneau with RNP technology, and such technology also may be useful at DCA and SAN.

Results for Sacramento indicate only limited benefits, but the weather and demand data used are both approximate. Improved demand data, especially, may result in improved benefits.

Noise Reduction Benefits. The results indicate only minor noise improvements are possible at DCA by using SV.

Business Aircraft Analysis. The business aircraft analysis indicates significant benefits from the lowering of minimums. The FAA Wide Area Augmentation System is intended to allow Cat I operations to any airport in the U.S., and Local Area Augmentation Systems should enable using CAT II and higher. However, a technology, such as SV, may be a practical necessity (or regulatory requirement) for safe IFR operations into regional airports when ILS-quality runway and taxi lights and markers are not available.

RECOMMENDATIONS FOR FUTURE RESEARCH

Confirm Airport Analysis Assumptions and Results. We encountered significant delays establishing contacts with FAA airport personnel. The result was a late start on the DCA model and an inability to coordinate and confirm results with airport personnel. The airport results must, therefore, be considered preliminary. With the models in hand, visiting the airports and reviewing the assumptions and methods would be very useful.

Complete the Airport List. We did not model Reno, nor did we update the San Francisco analysis. These are tractable analyses recommend for follow-on work.

Analyze Regional Carrier Benefits. Because of resource limitations, we did not analyze the regional airline benefits. The problem is developing a reasonable regional airline schedule. We had such a schedule in hand for busines aircraft from SATS research. If a reasonable schedule can be developed efficiently, an LMINET regional carrier network analysis would be straightforward.

Develop an Integer-Arithmetic Fluid Flow Delay Model. We found during this task that using the non-linear, real variable arithmetic queuing algorithm complicates modeling of individual airlines, non-equipped aircraft, and airline-unique minimums; requiring mathematical closure assumptions, and resulting in unavoidable closure errors. M/M/1 or similar non-linear queuing algorithms are necessary to accurately estimate delay when an airport is operating near capacity. When demand is either well below or well above capacity, as is the case at regional airports, a simple "fluid flow" algorithm should be adequate. The advantage of a fluid flow algorithm is that delay and queue calculations become simple counting problems, and we can use integer arithmetic to track airplanes. With a fluid flow queue we can easily track the aircraft of specific airlines or those with specific equipment, and, while assumptions will still be required regarding service priority in queues, we would eliminate the closure errors that exist with the current models.

Estimate Synthetic Vision Costs. The next effort should address the costs and benefit:cost ratios for SV technologies. Such analysis has been put off because of uncertainties in SV equipage. Equipage estimates should now be available at a level adequate for credible cost estimating.

Noise Reduction Analysis. The airports listed in Chapter 7, for which we have existing noise models, should be reviewed to identify airports with noise problems that can be improved by using SV.

Appendix A
Washington Reagan Airport Model

GENERAL COMMENTS WASHINGTON REAGAN AIRPORT (DCA)

Washington Reagan airport has three intersecting runways, a configuration we have not previously analyzed. The runway layout for DCA is shown in Figure A-1.

Figure A-1. Washington Reagan Airport Runway Layout

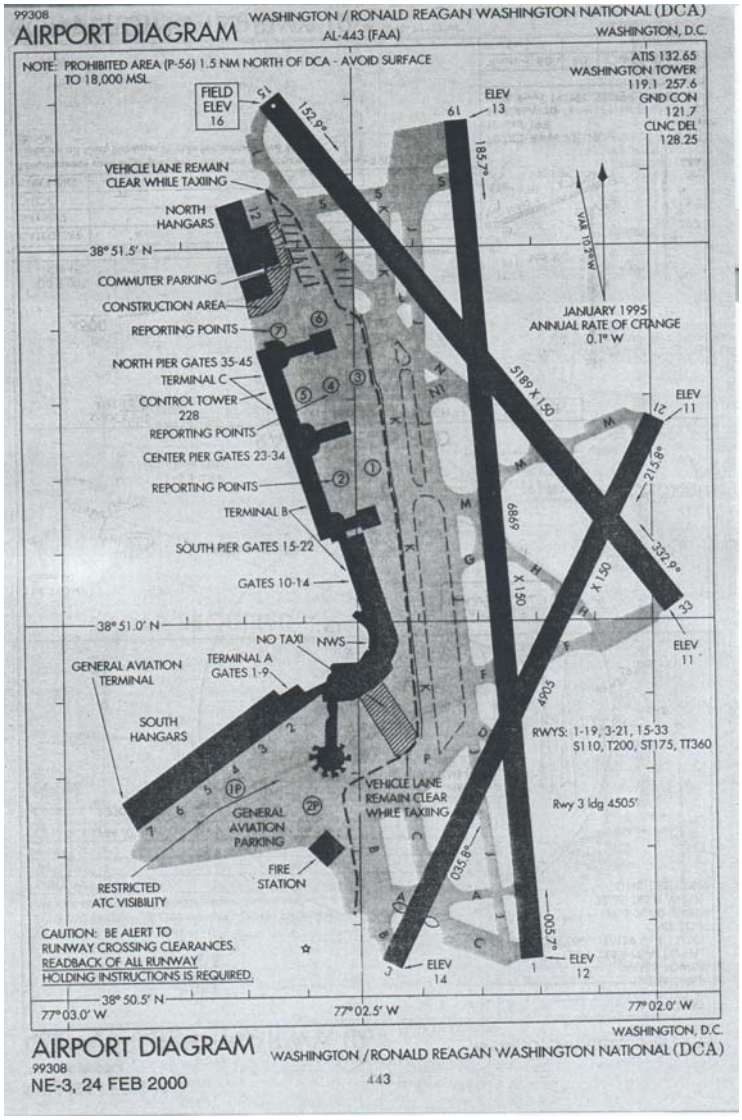

The prevailing winds at DCA are almost evenly split between north and south, as are operations. Because of restricted areas and obstructions in the north, the only ILS runway is Runway 1. Runway 1/19 is the longest runway with a length of only 6,869 feet. Runway 33/15 is the next longest at 5,189 feet and can support both propeller aircraft and jets. Runway 3/21, with a length of 4,905 feet and a displaced threshold in the 3 direction, is used for propeller aircraft only. As general policy, propeller aircraft are not offered Runways 1 and 19.

In ILS conditions the airport reverts to single-runway operation on Runway 1 (regardless of wind direction). At all other times the runways are used in a coordinated cyclic pattern. During our visit to DCA, we were told that the "standard" cycle for north flow is:

1. arrival on Runway 1,
2. departure on Runway 3,
3. departure on Runway 1,
4. departure on Runway 33, and
5. repeat.

DCA Capacity Model

All of our previous capacity models combined basic runway configurations[1] to generate the capacities for different airport configurations. In this model, we address the cyclic operation directly. Capacity points include maximum departures for three runways, maximum arrivals for two runways, the standard 1 arrival–3 departure (1A3D) cycle, and a 2 arrivals–1 departure (2A1D) cycle. We also developed the opposite direction arrival-departure cycle described in Appendix B. The standard 1A3D cycle can be used to demonstrate our modeling approach.

Description of the Standard 1A3D Cycle.

Figure A-2 is a time-distance diagram for the standard cycle. The abscissa represents both time and the runway threshold. The ordinate represents distance before and after the threshold. Starting from the left in the diagram, the cycle begins with arrival A1 crossing the threshold. After the arrival passes the 1–3 intersection the departure on Runway 3 is released. Once the Runway 3 departure passes the 3–1 intersection (or after the arrival clears the Runway 1, whichever is later), the departure on Runway 1 is released. Once the Runway 1 departure passes the 1–33 intersection, the Runway 33 departure is released. Finally, when the Runway 33

[1] We typically combine single-runway, intersecting-runway, and parallel dependent-runway configurations. For each configuration, we calculate capacity points for all-arrivals, all-departures, equal arrivals-departures, and free departures during all-arrivals.

departure passes the 33–1 intersection, the next arrival can land and repeat the cycle.

Figure A-2. DCA Standard 1A-3D Procedure for the North Flow

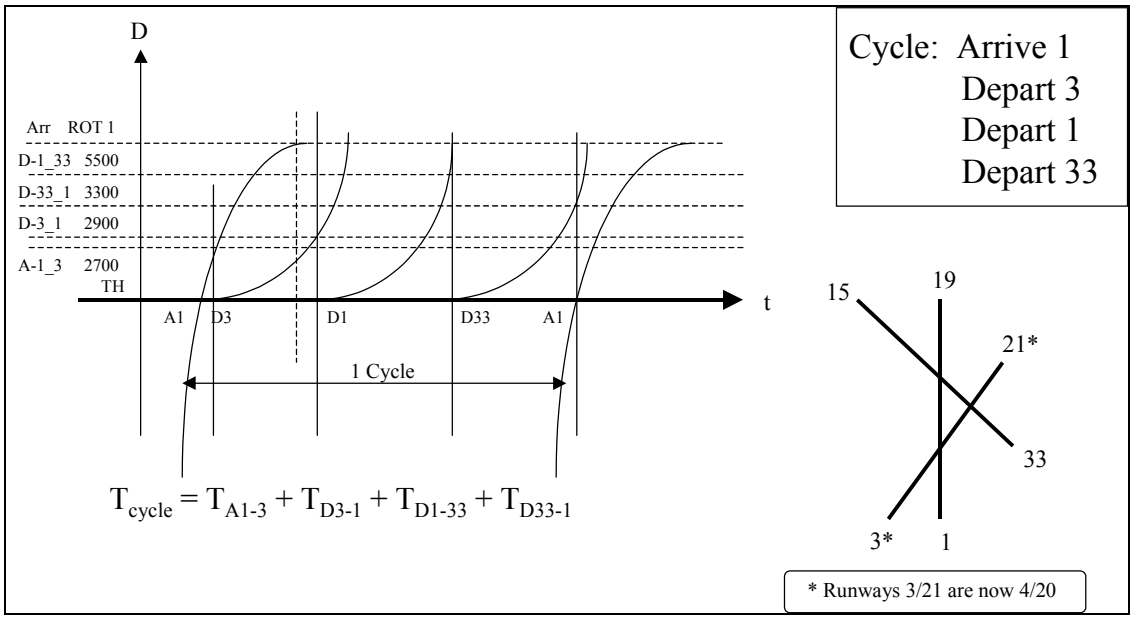

Equation 1 represents the cycle time for the process:

$$T_o = T_{A1-3} + T_{D3-1} + T_{D1-33} + T_{D33-1} \qquad \text{[Eq. A-1]}$$

where

T_o = the cycle time interval

$T_{A1\text{-}3}$ = the time for the arrival on 1 to clear the 1–3 intersection

$T_{D3\text{-}1}$ = the time for the departure on 3 to clear the 3–1 intersection

$T_{D1\text{-}33}$ = the time for the departure on 1 to clear the 1–33 intersection

$T_{D33\text{-}1}$ = the time for the departure on 33 to clear the 33–1 intersection

To determine the cycle time we needed to evaluate the intersection clearing times for the arrival and the departures.

Arrival Intersection Clearing Time

We calculated the intersection clearing times for arrivals using the touchdown speed, a constant deceleration, and the distance to clear the intersection. We assumed that touchdown occured a fixed distance from the threshold (typically 1,000 feet). Uncertainties are associated with all variables.

The distance covered decelerating from an initial touchdown speed is given by

$$x = V_0 t - \frac{1}{2} a t^2 \qquad \text{[Eq. A-2]}$$

where

x = the distance to clear the intersection

V_o = the touchdown speed

t = time

a = acceleration ($-a$ = deceleration)

This is a quadratic equation for t as a function of x. The solutions of the quadratic are

$$t = \frac{V_0}{a} \pm \sqrt{\frac{V_0^2}{a^2} - \frac{2x}{a}} \qquad \text{[Eq. A-3]}$$

There are two positive real roots. What they mean is, if we just let time roll on and on, the aircraft decelerating continuously, eventually stops and backs up. Thus, it reaches certain values of x twice. We obviously want the smaller root, so we take

$$t = \frac{V_0}{a} - \sqrt{\frac{V_0^2}{a^2} - \frac{2x}{a}} \qquad \text{[Eq. A-4]}$$

There is a limit, namely $x_{\max} \equiv \frac{1}{2}\frac{V_0^2}{a}$, to the distance x that the aircraft can reach. That's as far as the aircraft will roll; the program tests for this limit and reduces the deceleration if it is approached before the intersection is cleared.

Linearizing and ignoring higher-order terms, changes, δt, induced by δV_0, δa, and δx are given by

$$\delta t = \frac{\partial t}{\partial V_0}\delta V_0 + \frac{\partial t}{\partial a}\delta a + \frac{\partial t}{\partial x}\delta x \qquad \text{[Eq. A-5]}$$

where the δ's are all zero-mean normal random variables. In this case, t is a normal random variable with mean t_0,

$$t_0 \equiv \frac{V_{00}}{a_0} - \sqrt{\frac{V_{00}^2}{a_0^2} - \frac{2x_0}{a_0}} \qquad \text{[Eq. A-6]}$$

and variance,

$$Var(t) = \left(\frac{\partial t}{\partial V_0}\right)^2 \sigma_{V0}^2 + \left(\frac{\partial t}{\partial a}\right)^2 \sigma_a^2 + \left(\frac{\partial t}{\partial x}\right)^2 \sigma_x^2 \qquad \text{[Eq. A-7]}$$

The subscript "*0"* in the equation for the mean signifies that the mean values of the parameters are used to determine t_o. Properly, in each partial derivative below, V_0, a, and x should all have subscript "*0*" to indicate the use of mean values, but we leave them out for readability.

The partial derivatives are:

$$\frac{\partial t}{\partial V_0} = \frac{1}{a} - \frac{V_0}{a^2\sqrt{\frac{V_0^2}{a^2} - \frac{2x}{a}}} \qquad \text{[Eq. A-8]}$$

$$\frac{\partial t}{\partial a} = -\frac{V_0}{a^2} - \frac{1}{2}\frac{1}{\sqrt{\frac{V_0^2}{a^2} - \frac{2x}{a}}}\left[-\frac{2V_0^2}{a^3} + \frac{2x}{a^2}\right] \qquad \text{[Eq. A-9]}$$

$$\frac{\partial t}{\partial x} = \frac{1}{a\sqrt{\frac{V_0^2}{a^2} - \frac{2x}{a}}} \qquad \text{[Eq. A-10]}$$

Departure Intersection Clearing Time

The intersection clearing times for departures are calculated on the basis of a constant acceleration from zero speed, and the distance to clear the intersection. A time delay *cbar* is assumed between the departure clearance and the beginning of acceleration. The time delay is short if the aircraft is holding in position and longer if it is holding off the runway. As with the arrival, uncertainties are associated with all variables.

The distance covered accelerating from zero speed after an initial time delay is given by

$$x = \frac{1}{2}at^2 + cbar \qquad \text{[Eq. A-11]}$$

where

x = the distance to clear the intersection

a = the acceleration

t = the time to clear the intersection

cbar = is the initial delay

solving directly for t we have

$$t = \sqrt{\frac{2x}{a}} + cbar \qquad \text{[Eq. A-12]}$$

Again, linearizing and ignoring higher order terms we have

$$\delta t = \frac{\partial t}{\partial a}\delta a + \frac{\partial t}{\partial x}\delta x + \frac{\partial t}{\partial cbar}\delta_{cbar} \qquad \text{[Eq. A-13]}$$

As above, t is a normal random variable with mean

$$t_0 = \sqrt{\frac{2x_0}{a_0}} + cbar_0 \qquad \text{[Eq. A-14]}$$

and variance

$$Var(t) = \left(\frac{\partial t}{\partial a}\right)^2 \sigma_a^2 + \left(\frac{\partial t}{\partial x}\right)^2 \sigma_x^2 + \left(\frac{\partial t}{\partial cbar}\right)^2 \sigma_{cbar}^2 \qquad \text{[Eq. A-15]}$$

Here again, a and x in the equations below should properly have a "0" subscript to indicate the use of mean values, and we again leave them out for readability.

The partial derivatives are

$$\begin{aligned} \frac{\partial t}{\partial x} &= \sqrt{\frac{1}{4} \times \frac{2}{xa}} \\ \frac{\partial t}{\partial a} &= \sqrt{-\frac{1}{4} \times \frac{2x}{a^3}} \\ \frac{\partial t}{\partial cbar} &= 1 \end{aligned} \qquad \text{[Eq. A-16]}$$

In this case, the variance reduces to a relatively simple equation.

$$Var(t) = \frac{1}{4} \times \frac{2\sigma_x^2}{xa} - \frac{1}{4} \times \frac{2x\sigma_a^2}{a^3} + \sigma_{cbar}^2 \qquad \text{[Eq. A-17]}$$

Combining variables gives the following result.

$$Var(t) = \frac{1}{4} \times \frac{2x}{a} \times \left(\frac{\sigma_x^2}{x^2} + \frac{\sigma_a^2}{a^2}\right) + \sigma_{cbar}^2 \qquad \text{[Eq. A-18]}$$

Total Cycle Time

The mean and variance of the total cycle time is the sum of the means and variances of the individual arrival and departure clearance times.

Capacity Calculation

In the capacity model, we calculate clearing times and variances for arrivals and departures through all intersections for each class of aircraft. These times and their variances are combined to find the mean times and variances, by aircraft class, for the runway cycles that we're interested in.

We used modified versions of our previously developed capacity model functions get_arv_cap and get_dep_cap to calculate the capacity for each leg of the cycle using the aircraft mix appropriate for the particular leg.[2] For example, the arrival

[2] The modifications to the procedures enable inputting and using class-unique cycle-time variances.

capacity of Runway 1 in VFR weather is calculated using only jets, while the departure capacity of Runway 3 is calculated using only small aircraft and large-class turboprops. In the capacity procedures, the cycle time is treated as a super runway occupancy time (ROT). As discussed in previous reports[3] the capacity procedures determine the longest expected inter-arrival and inter-departure times subject to single-aircraft runway occupancy and miles-in-trail (MIT) constraints. In the case of the DCA cycles, the cycle-time/ROT is expected to control, but MIT is always checked. The cycle-time variances are used in the procedures to calculate standard deviations of interarrival and interdeparture times, which in turn are used to ensure 95 percent confidence of no violation of MIT spacing and 97.5 percent confidence of no runway incursion.

Once we determine capacities of the individual legs of the cycle, we use the lowest capacity (longest time) leg to determine the capacity of the whole cycle.

The all-arrival, all-departure, and 2A-1D configurations follow the same development as the standard cycle. We use a two-runway arrival cycle for the maximum arrival point instead of a three-runway point because the capacity calculated for the three-runway case exceeds, by far, the maximum capacity claimed by DCA personnel or found in FAA baseline estimates. Logically, the three-runway cycle, which requires extraordinary arrival coordination, three independent approach paths, and adequate taxi space for arrivals, could not be sustained at DCA.

The cycle-controlled procedures described above apply to conditions where all the runways are available. In the case of only a single runway being available, we use our basic single-runway algorithms.

Figure A-3 displays the baseline capacity frontiers we calculated for DCA. The chart indicates clearly how capacity at DCA decreases in inclement weather. When opposite direction operations are necessary, the capacity falls to the point labeled “Opposite.” Given that synthetic vision (SV) will support curved IFR approaches, the use of SV technology can keep capacity at the level of the upper curves, and eliminate the need for opposite-direction operations.

[3] *Estimating the Effects of the Terminal Area Productivity Program*, Lee et al, NASA CR-201682, April 1997, and

Benefit Estimates of Terminal Area Productivity Program Technologies, Hemm et al, NASA CR-1999-208989, Jan 1999.

Figure A-3. DCA Baseline Capacity Curves

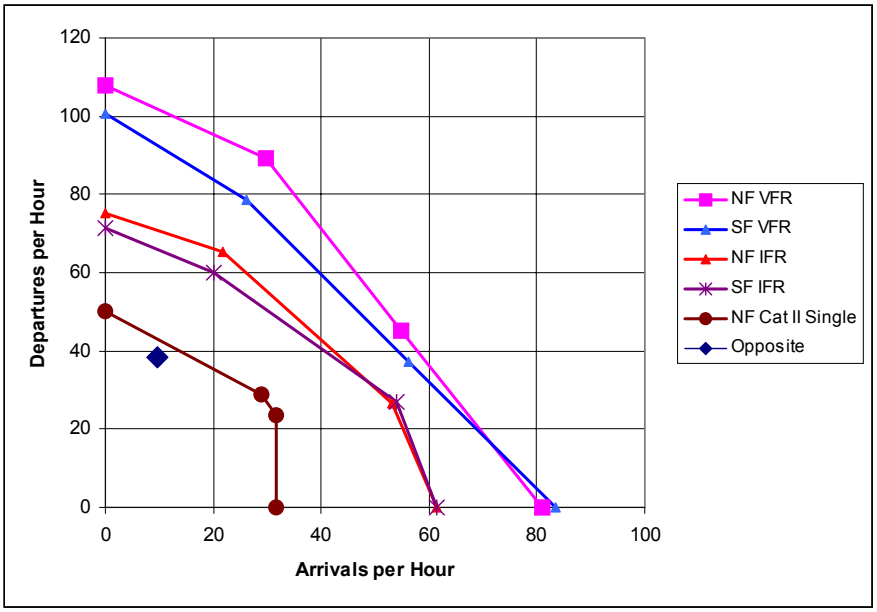

DCA Delay Model

The DCA delay model has some unique features, but is basically similar to our previously developed delay models. The delay model is still fundamentally an analytic model based on hourly aggregated demand and capacity, and uses an M/M/1 queuing algorithm.[4] The model steps through several years of weather data, hour-by-hour, checking the demand for the hour, and determining individually for arrivals and departures, the available capacity, the delay, the size of queues, and annual averages.

As with our other airport models, the DCA model includes specific logic for selection of configurations. At DCA, only two basic configurations are used, north flow and south flow. These configurations are selected according to wind direction. Our selection logic lets the configuration change with the wind. We tracked the wind history to check whether this logic would result in significant hourly (and unreasonable) flip-flopping of configurations. The results show that one-hour changes only occurred 999 times during of the 52,584 hours tracked. In 481 cases, the wind did not shift for 24 hours. Consequently, the simple wind-following selection is considered adequate. The wind-based selection results in an almost exact 50–50 split between North and South operations.

We have expanded the demand data, compared to past work, to model propeller-only and jet-only runways, and to determine, hourly, the need for opposite direction procedures. We still use the Official Airline Guide (OAG) and FAA Terminal Area Forecast to develop demand data, but, where in the past we developed repre

[4] M/M/1 signifies a Poisson arrival/Poisson service/single server queue.

sentative daily arrival and departure demand for summer and winter weekdays, Saturdays, and Sundays; in this task, we use the OAG to generate an expanded set of data for each hour of the year. The currently used data include aggregate arrival and departure demand, demand for specific aircraft weight classes and types (e.g., small-class jet and prop, large-class small jet and prop), the demand for a specific airline, and demand for departure stage lengths equal to or greater than 800, 1,000, and 1,200 miles. A one-day sample of the DCA demand data is shown below.

```
DCA demand file for 1997 and AA airline.
The parameters are:

M      H      arr d75   dsm  a75   asm dlt  dst alt  ast d10
   d       dep  dhv   dlg  ahv  alg  dlsj dsj alsj asj  d8  d12
1 1  100   0   4 0 0   0 0 0 0   4 0 0 0 0 0 0 1 0 0 0 0 0
1 1  200   0   0 0 0   0 0 0 0   0 0 0 0 0 0 0 0 0 0 0 0 0
1 1  300   0   0 0 0   0 0 0 0   0 0 0 0 0 0 0 0 0 0 0 0 0
1 1  400   0   0 0 0   0 0 0 0   0 0 0 0 0 0 0 0 0 0 0 0 0
1 1  500   0   0 0 0   0 0 0 0   0 0 0 0 0 0 0 0 0 0 0 0 0
1 1  600   0   0 0 0   0 0 0 0   0 0 0 0 0 0 0 0 0 0 0 0 0
1 1  700  13   0 0 4   9 0 0 0   0 0 2 2 0 0 0 0 0 0 3 3 1
1 1  800  11   5 0 1  10 0 0 1   4 0 0 3 0 0 0 1 0 0 3 1 0
1 1  900  14  19 0 0  13 1 0 0  17 2 0 1 0 1 1 1 0 2 3 1 0
1 1 1000  17  17 0 1  15 1 0 1  16 0 1 1 0 1 2 3 0 0 5 1 1
1 1 1100  18  12 0 1  16 1 0 1  10 1 3 2 0 1 2 1 0 1 2 0 0
1 1 1200  14  15 0 1  12 1 0 1  14 0 3 3 0 1 1 3 0 0 2 2 1
1 1 1300  13  17 0 1  12 0 0 1  12 4 0 4 0 0 1 3 0 4 2 1 0
1 1 1400  20  19 0 1  18 1 0 0  19 0 1 4 0 1 3 5 0 0 5 1 0
1 1 1500  18  16 0 0  17 1 0 0  15 1 1 5 0 1 2 3 0 1 1 1 1
1 1 1600  19  17 0 1  15 3 0 3  14 0 3 3 0 3 2 3 0 0 1 0 0
1 1 1700  18  20 0 1  17 0 0 1  19 0 3 5 0 0 0 6 0 0 2 2 1
1 1 1800  21  20 0 1  20 0 0 1  18 1 1 7 0 0 4 5 0 1 3 1 0
1 1 1900  14  23 0 1  12 1 0 0  21 2 3 2 0 1 4 2 0 2 1 0 0
1 1 2000  23  19 0 0  22 1 0 1  16 2 3 2 0 1 1 1 0 2 6 2 1
1 1 2100  21  19 0 1  17 3 0 0  19 0 1 4 0 3 1 5 0 0 0 0 0
1 1 2200   7  18 0 0   7 0 0 2  15 1 1 0 0 0 3 2 0 1 0 0 0
1 1 2300   0   9 0 0   0 0 0 2   6 1 0 0 0 0 0 1 0 1 0 0 0
1 1 2400   0   1 0 0   0 0 0 0   1 0 0 0 0 0 0 0 0 0 0 0 0
```

The consideration of opposite-direction operations was developed for DCA and also is used for San Diego. At DCA, when conditions require using Runway 1 with a tailwind, the demand data are checked for departures with stage lengths exceeding 1,000 miles. The fraction of those departures compared to the total departures for the hour is used to estimate the fraction of the hour that the opposite-direction arrival-departure procedure will be used.

SUMMARY AND FUTURE RESEARCH

The DCA model seems to provide reasonable results. The capacities generally agree with both the information received from DCA personnel and with the FAA Benchmark estimate[5] for DCA. Unfortunately, we only had a 2-hour meeting with DCA, and it would be fruitful in the future to schedule a new meeting to review the results and confirm the assumptions.

[5] *Airport Capacity Benchmark Report 2001*

Appendix B
Opposite-Direction Arrival-Departure Capacity Procedure

At both Washington Reagan (DCA) and San Diego (SAN), sometimes tailwind runways are the only ones open. At those times, aircraft departing on long trips requiring upwind departures, must take off directly into the arrival stream. We have not previously encountered this situation, so we had to develop new capacity algorithms. Synthetic vision could reduce the minimums on all runways, so that opposite-direction operations are no longer needed.

CYCLE DESCRIPTION

Figure B-1 is a diagram of the process. The diagram is a time-distance graph with time as the abscissa and distance as the ordinate. The two horizontal lines "N" and "S" represent the two thresholds of the runway. The process starts with the upwind departure starting from the "S" end of the runway and flying to a turn point a distance DX from the "N" end of the runway. At this point, for maximum capacity, the arrival is the minimum separation distance, SX, from the departure. The arrival flies the distance SX plus the distance DX to the runway, lands, and departs the runway at the end of its average runway occupancy time (ROT). At this time, a second upwind departure can leave.

Figure B-1. Opposite-Direction Arrival-Departure with Additional Downwind Departures

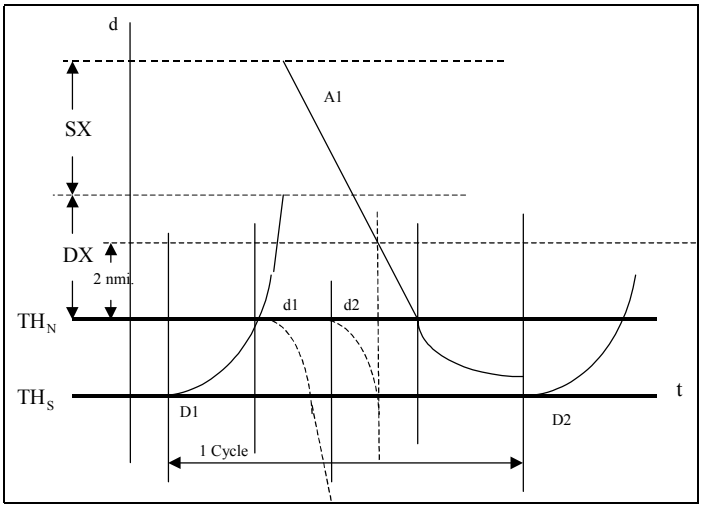

Downwind departures can take place during the interval between the time the upwind departure leaves the airport and the time the arrival crosses the threshold. In IFR conditions, the interval is reduced because FAA rules forbid releasing a departure when an arrival is within two miles of the threshold. The vertical dotted line represents the 2–mile limit.

ALGORITHM DESCRIPTION

The basic algorithm estimates the time for the departure to clear the runway and fly to the turn point, assuming acceleration at a fixed rate to a set speed limit followed by constant speed flight to the turn point. The arrival flies to the threshold at a constant speed and exits the runway after a set ROT. Equation B–1 represents the cycle time.

$$T_o = R_D + \frac{D_D}{V_D} + \frac{(D_D + S)}{V_A} + R_A + cbar \qquad \text{[Eq. B-1]}$$

where:

T_o = the cycle time interval

R_D = the upwind departure runway occupancy time

D_D = the upwind departure distance to turn

V_D = the average speed of the upwind departure after departing the runway

S = the minimum arrival-departure separation distance

V_A = the arrival average speed to the threshold

R_A = the arrival runway occupancy time

$cbar$ = the time between departure clearance and acceleration

Uncertainties are applied to all parameters and the resulting variance is used to ensure that the final inter-arrival and inter-departure time represents the 97.5 percent confidence level of no violation.

By linearizing and ignoring second-order terms we can write:

$$\delta t = \frac{\partial t}{\partial R_D}\delta_{R_D} + \frac{\partial t}{\partial D_D}\delta_{D_D} + \frac{\partial t}{\partial V_D}\delta_{V_D} + \frac{\partial t}{\partial V_A}\delta_{V_A} + \frac{\partial t}{\partial R_A}\delta_{R_A} + \frac{\partial t}{\partial cbar}\delta c_{cbar} \qquad \text{[Eq. B-2]}$$

Using Equation B–1 to find the partial derivatives we get:

$$\begin{aligned}
\frac{\partial t}{\partial R_D} &= 1 \\
\frac{\partial t}{\partial D_D} &= \frac{1}{V_D} + \frac{1}{V_A} \\
\frac{\partial t}{\partial V_D} &= -\frac{D_D}{V_D^2} \\
\frac{\partial t}{\partial V_A} &= -\frac{(D_D + S)}{V_A^2} \\
\frac{\partial t}{\partial R_A} &= 1 \\
\frac{\partial t}{\partial cbar} &= 1
\end{aligned} \qquad \text{[Eq. B-3]}$$

Recalling that the variance of a sum is the sum of the variances of its terms, we have

$$\text{var} = \sigma_{R_D}^2 + \left[\frac{1}{V_D} + \frac{1}{V_A}\right]^2 \sigma_D^2 + \left[\frac{-D_D}{V_D^2}\right]^2 \sigma_{V_D}^2 + \left[\frac{-(D_D + S)}{V_A^2}\right]^2 \sigma_{V_A}^2 + \sigma_{R_A}^2 + \sigma_{cbar}^2 \quad \text{[Eq. B-4]}$$

Using our standard assumption that the controller generates sufficient spacing to assure a 97.5 percent probability of no runway incursion (i.e., *To* + 2.125 times the standard deviation), we estimate the cycle time with Equation B-1 and the variance as follows:

$$cycle\_time = R_D + \frac{D_D}{V_D} + \frac{(D_D + S)}{V_A} + R_A + cbar + 2.215\sqrt{\text{var}} \qquad \text{[Eq. B-5]}$$

The runway can sustain one arrival and at least one departure per cycle, so the hourly capacity, is *60/cycle-time* when cycle time is calculated in minutes.

Similarly, the time available for the downwind departures with and without the 2-mile limit can be estimated. In both cases, the time is estimated without the departure and arrival ROTs. In the latter case, the arrival flight distance is reduced by 2 miles, and the term (D_D+S) is replaced by (D_D+S-2).

The time required for a downwind departure is estimated using the standard get_dep_cap procedure and the largest integer number of departures achievable in the available interval is added to the upwind departure to give the total departures for the cycle.

Input Parameters

All input parameters are constants except the departure runway occupancy time, R_D, and the average speed to the departure turn, V_D, which are calculated. For these two parameters, the assumption is that the departing aircraft accelerates at a constant rate up to a pattern limit speed and continues at that speed. The time and distance to reach the limit speed is calculated, along with the time and distance needed to cover the runway distance. The runway distance and runway time are used to calculate the ROT. The post-runway acceleration distance is subtracted from the departure turn distance to find the constant-speed departure distance. The constant speed departure distance and pattern limit speed are used to find the time flown at constant speed. Finally, the post-runway acceleration time and constant-speed time are divided into the departure turn distance to give the average post-runway departure speed, V_D. Both the acceleration, a_D, and pattern limit speed, V_{limit} are input as constants.

Table B-1 shows the typical values used for the input parameters. In the computer procedure, times are calculated for each combination of arrival and departure aircraft class, and some parameters, such as ROT have different values for each aircraft class.

Table B-1. Input Parameters

Parameter	Mean value	Standard deviation	Units
D_D	3.5	0.25	nautical miles
a_D	0.2	0.02	g's
V_{limit}	240	5	knots
S	3.0	0.25	nautical miles
V_A	135-145	5	knots
R_A	0.5-1.0 / 30-60	0.13 / 8	minutes/seconds
cbar	0.25 / 15	0.025 / 1.5	minutes/seconds

Results

The results, for parameters such as those in Table B-1, are about 10 arrivals and 40 departures per hour if 10 departures are upwind and 30 downwind.

For estimating the capacity for a particular hour, we determined the fraction of long-range departures that needed to depart upwind and assumed opposite-direction operations will be used for that fraction of the hour. The remainder of the hour has the best capacity appropriate for the weather conditions. Capacity can be improved by banking arrivals and departures, and we recommend determining practice at specific airports as a subject for future research.

Appendix C
Single-Runway Capacity and Delay Models

This appendix describes the features of the single runway models we developed during this task. In our previous work, the emphasis has been on estimating the ability of synthetic vision (SV) technology to reduce general delay at the busiest airports in the nation. In the current task, the emphasis has shifted to smaller airports that have unique features, such as difficult terrain. Several of these airports have only one runway. Also, interest exists in determining the benefits accruing to a specific airline at an airport. Finally, interest exists in modeling additional problems such as missed approaches. We developed the new single runway capacity and delay models to address these issues.

MODEL DESCRIPTION

In addition to the basic capacity parameters and airport minimums the single runway models have features that can

- Calculate delays for a specific airline,
- Remove non-equipped aircraft from the demand,
- Calculate the effect of missed approaches,
- Calculate the effect of opposite-direction arrivals and departures, and
- Calculate the effect of changes in taxi and turn-around time.

The single-runway capacity model is essentially unchanged from our standard capacity models except for the addition of the opposite-direction arrival-departure algorithm. On the other hand, we significantly modified the delay model.

The delay model is still fundamentally an analytic model based on hourly aggregated demand and capacity, and uses an M/M/1 queuing algorithm.[1] The model steps through several years of weather data, hour-by-hour, checking the demand for the hour, and determining individually for arrivals and departures, the available capacity, the delay, the size of queues, and the annual averages.

The queuing algorithm uses aggregate arrival and departure data and generates aggregate delay and queue information. Tracking the delays for an individual airline requires that we track the number of airline aircraft in the demand and in the

[1] M/M/1 signifies a Poisson arrival/Poisson service/single server queue.

arrival and departure queues; data that are not available from the queuing algorithm, and must, therefore, be approximated. We note the approximation schemes in the procedure discussed below.

When tracking airline delays we keep track of the airline's aircraft as they arrive and require that an aircraft be available before a departure can occur. We specifically assume that any airline aircraft can support any departure. This assumption is valid for operations in which aircraft are turned around for immediate departure.

As with past models, we do not cancel flights. Analyzing canceled flights is possible; however, to date, no reliable logic, such as canceling after X hours of delay, exists to determine when flights would be canceled.

DEMAND DATA

In comparison with our previous work, we have expanded the demand data. We still use the Official Airline Guide (OAG) and FAA Terminal Area Forecast (TAF) to develop demand data, but, in the past we developed representative daily arrival and departure demand for summer and winter weekdays, Saturdays, and Sundays. In this task, we use the OAG to generate an expanded set of data for each hour of the year. The current demand data includes not only the aggregate arrival and departure demand, but also the demand by aircraft weight class and type (jet, turboprop, or piston), the demand by specific airline, and, if necessary, demand by departure stage length.

We generate the demand data from the OAG in four steps. First, we load the monthly OAG flight schedules into a MS Access database. Second, we use queries to generate tables containing the desired data such as departure airport, departure time, equipment, arrival airport, arrival time, and flight number. Separate queries are run for the airport as the origin and as the destination. The data includes the parameter "eday," which is a 31–character binary string that represents the days of the month. The first position is the 1st of the month and so on through the 31st day. A "1" in eday signifies that the flight occurs on that day and a "0" indicates no flight. Short months, obviously have 0's in the last positions. In the third step, we convert the Access tables to text documents and combine the arrival and departure data for each month. In the fourth step, we use a Pascal program to step through the data by flight, decode the eday parameter, determine the aircraft classes according to weight, calculate hourly demands, and produce an hourly demand schedule for the year. The following sample is the first day's demand for the San Diego airport and American Airlines.

M	D	Hour	arr	aAL	aALsP	dB75	dsml	aB75	asml	asmlP
			dep	dAL	dALsP	dhvy	dlrg	ahvy	alrg	dsmlP
1	1	100	0	3	0	1	0	0	0	0
1	1	200	0	0	0	0	0	0	0	0
1	1	300	0	1	0	0	0	0	0	0
1	1	400	0	0	0	0	0	0	0	0
1	1	500	0	0	0	0	0	0	0	0
1	1	600	0	0	0	0	0	0	0	0
1	1	700	11	0	2	0	0	0	0	0
1	1	800	19	4	3	1	0	0	1	0
1	1	900	22	3	3	1	0	0	0	0
1	1	1000	13	13	1	1	0	0	1	0
1	1	1100	13	15	2	1	0	0	0	0
1	1	1200	13	20	0	2	0	0	0	0
1	1	1300	20	13	3	2	0	0	0	0
1	1	1400	15	19	1	3	0	0	0	0
1	1	1500	12	13	1	2	0	0	0	0
1	1	1600	14	11	1	1	0	0	0	0
1	1	1700	14	14	2	1	0	0	0	0
1	1	1800	16	18	1	3	0	0	1	0
1	1	1900	13	14	1	2	0	0	2	0
1	1	2000	14	21	1	2	0	0	1	0
1	1	2100	12	18	1	3	0	0	0	2
1	1	2200	10	16	2	2	0	0	0	0
1	1	2300	6	15	1	1	0	0	0	2
1	1	2400	1	2	0	1	0	0	0	0

MODEL OPERATION

The process flow of the delay model is as follows:

- Read the demand data[2]
- Scale the demand by the TAF factor.
- Accumulate the demands for later averaging
- Calculate running averages of the ratio of airline demand to total demand for closure calculations
- Identify and remove non-equipped aircraft from arrival and departure demand
- Calculate arrival and departure capacities for the hour on the basis of weather, wind and the departure to arrival demand ratio (including residual queues)
- Adjust the arrival demand (up) for missed approaches

[2] Current data includes: month, day, hour, total departure demand, total arrival demand, specific airline (AL) departure demand, AL arrival demand, AL small-propeller departure, AL small-propeller arrivals, heavy departures, B757 departures, large departures, small departures, heavy arrivals, B757 arrivals, large arrivals, small arrivals, small-propeller departures, and small-propeller arrivals. For DCA we add departures for specific stage lengths.

- Adjust the arrival capacity for opposite-direction arrival-departure operations
- Use the queuing algorithm to calculate the delay and residual arrival queue length
- Determine the airline arrival delay per flight from the delay, divided by the demand plus the change in the queue length. For this we need the airline fraction of new demand, which is found easily from the demand input, and the airline fraction of the old queue, which is more difficult to find.
  - Find the number of arrival aircraft served from the queue and from the current demand using one of the following approximations:
    - First-in-first-out (FIFO) service (currently used), in which aircraft in the queue are assumed to be served before the new demand
    - Proportional service, in which aircraft in the queue and the current demand are assumed served on the basis of the fractions of queue and new demand in the total demand.
  - Update the number of airline aircraft in the residual arrival queue according to the running average of airline aircraft in the arrival demand—this is a closure approximation.
  - Calculate the number of airline aircraft serviced from the new arrival demand according to the total new arrival demand serviced and the fraction of airline aircraft in the demand.
- Calculate the number of airline aircraft serviced from the last hour's queue according to the total number of arrival queue aircraft serviced and the fraction of airline aircraft in the queue.
- Add the airline aircraft serviced during the hour to the pool of airline aircraft available for departure. Arrivals are added in the current hour if taxi and turn-around times plus average arrival delay per flight for the hour are less than 1 hour, otherwise the arrival is added to the pool for the following hour.
- Determine the total departure demand on the basis of the total demand, the airline demand, and the number of aircraft available to fill the airline demand. If the airline does not have enough aircraft, the total demand for the hour is reduced, an hour of delay per shortfall is added, and the unsatisfied demand is passed to the next hour.
  - Adjust departure capacity for missed approaches.
  - Adjust departure capacity for opposite direction arrivals and departures

- ➢ Calculate the departure delay and the residual departure queue
- ➢ Determine the airline departure delay per flight from the delay, divided by the demand plus the change in queue length.
    - ■ Find the number of departure aircraft served from the queue and from the current demand using either FIFO or proportional service
    - ■ Update the number of airline aircraft in the residual departure queue on the basis of the running average of airline aircraft in the departure demand – this is a closure approximation.
    - ■ Calculate the number of airline aircraft serviced from the new departure demand on the basis of the total new departure demand serviced and the fraction of airline aircraft in the demand.
    - ■ Calculate the number of airline aircraft serviced from the last hour's queue on the basis of the total number of departure queue aircraft serviced and the fraction of airline aircraft in the queue.
    - ■ Accumulate delays
    - ■ Rename current hour delays and queues as previous hour delays and queues and step to the next hour
    - ■ At the end of the day, reset the delay parameters and the restock the departure pool to the original value. Continue the queues, unsatisfied departure demand, and departure aircraft available to the next day.

Choosing the FIFO or proportional service is required because analytic queuing algorithms such as ours do not track individual aircraft. A closure approximation must be used because the queuing algorithm is non-linear and generates errors when aircraft are removed from the queue and later added back. The airplane pool must be restocked daily because the OAG demand data generally does not have equal numbers of arrival and departures.

MODEL USE

The model operates the same as previous models in that we made separate runs for each technology and demand year. We used simple batch programs to automatically run through the four technologies and the eleven demand years from 2005 through 2015.

The major change for the current analysis is that we must make preliminary runs to set the size of the initial departure pool. We set the pool size to a level that produces no delays caused by unavailable aircraft during VFR conditions. The model includes flags to force all-VFR conditions.

The model also has a flag to define the total airport demand as one airline. Setting this flag and inputting a very large departure pool results in a delay analysis identical to those used in previously work.

Appendix D
Economic Values for Benefit Analysis

In this task, for the airport benefit estimates, we use the same values for air carrier cost per minute of delay that we used in our previous study. We used the average of two values of cost per minute of delay. The lower of the two includes only variable operating cost (VOC) minus fuel and plus flight attendant costs (VOC-F+FA). The higher of the two is direct operating cost which includes both capital depreciation and fuel plus flight attendant costs (DOC+FA). The DOC and VOC define upper and lower bounds on the cost of delay. As before, we use the 1998 VOC-F+FA and DOC+FA values reported in the NASA Aviation Systems Analysis Capability (ASAC) report, *Cost and Operational Data - Equipment Level*. The values from ASAC are $44.71 per minute for DOC+FA and $27.15 per minute for VOC-F+FA in 1998 dollars. Using a 2.2 percent inflation factor from the 2000 President's Economic Report[1] we produce a DOC+FA value of $45.69 and a VOC-F-FA value of $27.75 in 1999 dollars. We used the average of the DOC+FA and VOC-F+FA costs for the summary savings. We also calculate discounted savings for a 1999 base and 7 percent discount factor and inflated (i.e., Then Year or Budget) savings for a 2.6 percent inflation rate.

We developed a regional air carrier cost per hour of delay for the business aviation analysis. Ground delay is the appropriate cost measure, because we assume that carriers take delays for closed destination airports on the ground at the departure airport. We developed the costs from Department of Transportation regional aircraft operating expense data.[2] For ground delay, we included aircrew, maintenance, and depreciation or rental costs, and excluded fuel and "other" costs. We specifically used the averaged values for 16-passenger aircraft. The result is a cost of $370 for each hour of ground delay in 1997 dollars. Escalating to 1999 dollars, using a 2.2 percent rate, gives $386 per hour.

We did not consider passenger time costs in our analyses. The FAA has recommended a value of $37.50 per hour per person in 1995 dollars for General Aviation business passengers.[3] This value is from the FAA's 1998 report*, Economic Values for Evaluation of FAA Investment and Regulatory Programs*. Interestingly, the corresponding value from the *1989* report is $37.06. If we assume eight passengers per plane, we get $300 dollars per hour of aircraft delay with the $37.50

[1] Table B-6, *Changes in special consumer price indexes, 1960-99*; All items (CPI-U), Year-to-year value

[2] Data from 1997 Bureau of Transportation Statistics Form 298-C, Schedule F*, Report of Aircraft Operating Expenses and Related Statistics*.

[3] Table 1-1, Recommend Hourly Values of Travel Time Savings*, Economic Values for FAA Investment and Regulatory Programs*, FAA-APO-98-8, June 1988.

value. Development of supportable costs for passenger delay should be a topic of future research.

Appendix E
Abbreviations

ANP	actual navigation performance
ASAC	Aviation System Analysis Capability
DOC	direct operating cost
EV	enhanced vision
FAA	Federal Aviation Administration
FIFO	first-in-first-out
FLIR	forward-looking infrared
GA	general aviation
GPS	Global Positioning Satellite
IFR	instrument flight rules
ILS	instrument landing system
INM	Integrated Noise Model
LMINET	A queuing network model of the U.S. national airspace
MIT	miles-in-trail
NASA	National Aeronautics and Space Administration
OAG	Official Airline Guide
RNP	required navigation performance
ROT	runway occupany times
RVR	runway visual range
SATS	Small Aircraft Transportation System
SV	synthetic vision
TAF	terminal area forecast
VFR	Visual Flight Rules
VOC	variable operating cost

REPORT DOCUMENTATION PAGE

Form Approved
OPM No.0704-0188

1. AGENCY USE ONLY *(Leave Blank)*	2. REPORT DATE	3. REPORT TYPE AND DATES COVERED
	June 2001	Contractor Report

4. TITLE AND SUBTITLE
Additional Benefit Estimates of Synthetic Vision Technology

5. FUNDING NUMBERS
POL 70525D

6. AUTHOR(S)
Robert Hemm, David Lee, Virginia Stouffer, and Ashleigh Gardner

7. PERFORMING ORGANIZATION NAME(S) AND ADDRESS(ES)
Logistics Management Institute
2000 Corporate Ridge
McLean, VA 22102-7805

8. PERFORMING ORGANIZATION REPORT NUMBER
LMI– NS014S1

9. SPONSORING/MONITORING AGENCY NAME(S) AND ADDRESS(ES)
National Aeronautics and Space Administration
Langley Research Center
Hampton, VA 23681-0001

10. SPONSORING/MONITORING AGENCY REPORT NUMBER
NASA CR

11. SUPPLEMENTARY NOTES
Langley Technical Monitor. Dan Williams
Final Report

12a. DISTRIBUTION/AVAILABILITY STATEMENT
Unclassified-Unlimited

12b. DISTRIBUTION CODE

The subject report documents additional research into the potential economic benefits of Synthetic Vision (SV) technology. While SV is primarily a safety program, it also allows reductions in delays by improving operations in poor weather. Previous work examined the benefits of SV at 10 major airports. The current reseach examines benefits at five additional airports: Juneau, San Diego (SAN), Washington Reagan (DCA), Sacramento (SMF) and Eagle County/Vail (EGE). Results indicate that significant benefits are possible for SAN through use of reduced minimums. Significant benefits are also possible for DCA through use of curved IFR approaches and reduced minimums. Benefits were noticible, but not dramatic, at SMF. Analysis of EGE was performed with a modified delay model due to the lack of significant scheduled demand at EGE. Use of SV at EGE can dramatically improve access, again through use of reduced minimums.
In addition to single airport analyses, the SV impact on business travel was estimated using a modified LMINET netwoek model and the Small Aircraft Transportation System (SATS) network of 2865 airports. A baseline analysis identified the top 100 delay airports in the SATS network and estimated the benefits of upgrading those 100 airports to Cat I, and Cat II instrument capability. The benefits of doing the same at all the SATS airports was also calculated.
Finally, a noise impact analysis was performed for DCA. Modest noise improvements are predicted for movement of all flights to the VFR river routes.

14. SUBJECT TERMS	15. NUMBER OF PAGES
Synthetic Vision, Benefit Analysis, Airport Capacity, Airport Delay	16. PRICE CODE

17. SECURITY CLASSIFICATION OF REPORT	18. SECURITY CLASSIFICATION OF THIS PAGE	19. SECURITY CLASSIFICATION OF ABSTRACT	20. LIMITATION OF ABSTRACT
Unclassified	Unclassified		UL